

CONCEPTUAL DESIGN OF A STEALTH UNMANNED COMBAT AERIAL  
VEHICLE WITH MULTIDISCIPLINARY DESIGN OPTIMIZATION

A THESIS SUBMITTED TO  
THE GRADUATE SCHOOL OF NATURAL AND APPLIED SCIENCES  
OF  
MIDDLE EAST TECHNICAL UNIVERSITY

BY

UĞUR ÇAKIN

IN PARTIAL FULFILLMENT OF THE REQUIREMENTS  
FOR  
THE DEGREE OF MASTER OF SCIENCE  
IN  
AEROSPACE ENGINEERING

JANUARY 2018



Approval of the thesis:

**CONCEPTUAL DESIGN OF A STEALTH UNMANNED COMBAT AERIAL  
VEHICLE WITH MULTIDISCIPLINARY DESIGN OPTIMIZATION**

submitted by **UĞUR ÇAKIN** in partial fulfillment of the requirements for the degree  
of **Master of Science in Aerospace Engineering Department, Middle East  
Technical University** by,

Prof. Dr. Gülbin Dural Ünver  
Director, Graduate School of **Natural and Applied Sciences**

\_\_\_\_\_

Prof. Dr. Ozan Tekinalp  
Head of Department, **Aerospace Engineering**

\_\_\_\_\_

Prof. Dr. Hüseyin Nafiz Alemdaroğlu  
Supervisor, **Aerospace Engineering Dept., METU**

\_\_\_\_\_

**Examining Committee Members:**

Prof. Dr. Serkan Özgen  
Aerospace Engineering Dept., METU

\_\_\_\_\_

Prof. Dr. Hüseyin Nafiz Alemdaroğlu  
Aerospace Engineering Dept., METU

\_\_\_\_\_

Prof. Dr. Altan Kayran  
Aerospace Engineering Dept., METU

\_\_\_\_\_

Assoc. Prof. Dr. Ali Türker Kutay  
Aerospace Engineering Dept., METU

\_\_\_\_\_

Assoc. Prof. Dr. D. Sinan Körpe  
Aerospace Engineering Dept., THK

\_\_\_\_\_

**Date:** 30.01.2018

**I hereby declare that all the information in this document has been obtained and presented in accordance with academic rules and ethical conduct. I also declare that, as required by these rules and conduct, I have fully cited and referenced all material and results that are not original to this work.**

Name, Last Name:

Signature:

## ABSTRACT

### CONCEPTUAL DESIGN OF A STEALTH UNMANNED COMBAT AERIAL VEHICLE WITH MULTIDISCIPLINARY DESIGN OPTIMIZATION

Çakın, Uğur

M.S., Department of Aerospace Engineering

Supervisor : Prof. Dr. H. Nafiz Alemdaroğlu

January 2018, 54 pages

The present study aims to develop a methodology for multi-disciplinary design optimization (MDO) of an unmanned combat aerial vehicle. At the current stage of optimization study, three disciplines are considered, which are aerodynamics, structural weight and radar cross section (RCS) signature. As objective functions, maximum range and minimum RCS signature are employed. To generate pareto-optimal solutions, multi-objective particle swarm optimization (MOPSO) function of MATLAB® is performed. To get aerodynamic coefficients of generated UCAV geometries, a high-fidelity aerodynamic analysis tool SU2 is employed. Moreover, to shorten computational effort, firstly, a meta-model for aerodynamic results is formed by performing multivariate adaptive regression splines (MARS) approximation. Structural and system weights are estimated by using statistical weight equations. After that, by using aerodynamic coefficients and estimated total weight, range is calculated. RCS signature values are calculated by conducting POFACETS which is an implementation of the physical optics approximation for predicting RCS of complex objects. Also, meta-model of RCS results is generated for decreasing the computational time. Finally, the developed framework is performed to optimize a UCAV planform as an example of the

framework's capability. The pareto-front results for MDO computations are presented in detail at results and discussion.

**Keywords:** Unmanned Combat Aerial Vehicle, Multidisciplinary Design Optimization, Multi-Objective Particle Swarm Optimization, Meta-Modelling, Conceptual Design.

## ÖZ

### ÇOK DİSİPLİNLİ TASARIM OPTİMİZASYONU İLE DÜŞÜK RADAR İZİNE SAHİP MUHARİP İHA KONSEPT TASARIMI

Çakın, Uğur

Yüksek Lisans, Havacılık ve Uzay Mühendisliği Bölümü

Tez Yöneticisi : Prof. Dr. H. Nafiz Alemdaroğlu

Ocak 2018, 54 sayfa

Bu tezde, muharip insansız hava aracının (MİHA) çok disiplinli tasarım optimizasyonu için bir metodoloji geliştirilmesi amaçlanmaktadır. Optimizasyon çalışmasının şu andaki aşamasında aerodinamik, ağırlık kestirimi ve radar kesit alanı (RKA) izi gibi üç disiplin ele alınmaktadır. Amaç fonksiyonları olarak, maksimum menzil ve minimum RKA izi kullanılmaktadır. Pareto-optimal çözümleri üretmek için çok amaçlı parçacık sürü optimizasyonu (ÇAPSO) yöntemi uygulanmaktadır. Oluşturulan MİHA geometrilerinin aerodinamik katsayılarını elde etmek için yüksek doğruluğa sahip bir aerodinamik analiz aracı SU2 kullanılmaktadır. Burada, hesaplama zamanını kısaltmak için Multivariate Adaptive Regression Splines (MARS) yaklaşımıyla aerodinamik sonuçlar için bir meta model oluşturulmaktadır. Yapısal ve sistem ağırlıkları istatistiksel ağırlık denklemleri kullanılarak hesaplanmaktadır. Hava aracı menzil hesabı, aerodinamik katsayılar ve tahmini toplam ağırlık kullanılarak yapılmaktadır. RKA izi değerleri, karmaşık nesnelerin RKA'sını tahmin etmek için fiziksel optik yaklaşımın bir uygulaması olan POFACETS kodu yardımıyla hesaplanmaktadır. Burada, hesaplama süresini azaltmak için RKA sonuçlarının meta-modeli oluşturulmuştur. Bunların sonunda, tasarım aracının kapasitesinin bir örneği olarak MİHA dış geometrisinin

optimizasyonu belirlenen amaç fonksiyonları için tasarım aracı kullanılarak yapılmıştır. Çok disiplinli tasarım optimizasyonu sonucu bulunan Pareto-optima sonuçları çalışma sonunda verilmektedir.

**Cpcj wt" Mgrlo ggt:** Muharip İnsansız Hava Aracı, Multidisipliner Tasarım Optimizasyonu, Parçacık Sürü Optimizasyonu, Meta-Modelleme, Kavramsal Tasarım

*“If I have seen further,  
It is by standing on the shoulders of giants”*  
**Sir Isaac Newton**

## ACKNOWLEDGEMENTS

I would like to express my deepest gratitude to my supervisor, Prof. Dr. H. Nafiz Alemdarođlu for his guidance, advice, criticism, insight, and encouragement throughout the research.

I want to express my gratitude to my colleagues, Ethem Hakan Orhan, Halil Kaya, Orkun ŐimŐek, Senem AyŐe Haser, Ceren Orhan, Huseyin Aktan, Hakan Tiftikçi, Tuđba Yıldırım, Tuđrul Yıldırım, Aykut Kutlu and my other friends who were there to give me support and advice during my study.

I want to express my deepest gratitude to my fellows, Durukan Tamkan, Hasan Őener, Ali Ünal, Ali Yıldırım, Mustafa İćen who give me strength to live in Ankara.

I would like to thank my parents and my wife who never ceased to give me encouragement and pray for me during my graduate study.

## TABLE OF CONTENTS

ABSTRACT .....	v
ÖZ .....	vii
ACKNOWLEDGEMENTS .....	x
TABLE OF CONTENTS .....	xi
LIST OF TABLES .....	xiii
LIST OF FIGURES .....	xiv
LIST OF SYMBOLS .....	xvi
LIST OF ABBREVIATIONS .....	xviii
CHAPTERS	
1. INTRODUCTION.....	1
1.1 Description of Unmanned Combat Aerial Vehicles (UCAV).....	1
1.2 Literature Review .....	3
1.3 Aim of this study .....	6
1.4 Outline of the presented work .....	6
2. DEVELOPMENT OF OPTIMIZATION FRAMEWORK .....	7
2.1 General Description of Framework.....	7
2.2 Aerodynamic Module.....	13
2.3 Radar Cross Section (RCS) Module .....	17
2.4 Weight Estimation Module .....	20
2.5 Optimization Module .....	23
3. RESULTS AND DISCUSSIONS .....	27
3.1 Results .....	27
3.2 Discussions.....	32
4. CONCLUSIONS AND FUTURE WORK .....	41
4.1 Conclusions .....	41
4.2 Future Work .....	43
REFERENCES.....	45

APPENDICES

A. META-MODELLING TECHNIQUE .....	49
B. VALIDATION OF MOPSO ALGORITHM FOR MULTIDISCIPLINARY OPTIMIZATION PROBLEM.....	53

## LIST OF TABLES

### TABLES

Table 2.1 Design variables and assumptions .....	9
Table 2.2 The lower and upper bounds of design space .....	10
Table 2.3 Actual and estimated weights .....	22
Table 2.4 The pseudocode of general MOPSO algorithm .....	26
Table 2.5 The optimization problem formulation .....	26
Table 3.1 Optimization parameters .....	27
Table 3.2 Change of geometry planform from min. PoD to max. Range .....	34
Table 3.3 Specifications of design point “Rep_50” geometry .....	38
Table B.1 Formulations of ZDT1 and MOP2 test functions.....	53

## LIST OF FIGURES

### FIGURES

Figure 1.1 Example of UCAVs in the world. (Left upper: BAE Systems Taranis [2], Right upper: Dassault nEUROn[3], Left lower: Northrop Grumman X-47B[4], Right lower: Boeing X-45A[5]) .....	2
Figure 1.2 SEAD/DEAD mission [1].....	3
Figure 1.3 UCAV Design mission [6].....	3
Figure 2.1 General scheme of optimization framework.....	8
Figure 2.2 SACCON 1303 geometry [6] .....	9
Figure 2.3 The parameterization of SACCON 1303 geometry.....	9
Figure 2.4 RCS signature of example UCAV in both polar (left) and linear (right) plots .....	12
Figure 2.5 Methodology of creating aerodynamic meta-model.....	14
Figure 2.6. Overview of mesh density .....	15
Figure 2.7 Pressure distribution for one of the sample UCAV geometry .....	16
Figure 2.8 Target model defined by using of triangular facets .....	18
Figure 2.9 The meta-modeling process of RCS analysis .....	19
Figure 2.10 The polar plot of RCS signature .....	20
Figure 2.11 Thrust vs. Engine weight relationship .....	22
Figure 2.12 Swarm behavior of birds [32] .....	24
Figure 2.13 PESA's archive generation .....	25
Figure 3.1 Trials for repository size. a) Repository size: %20 population size, b) Repository size: %30 population size, c) Repository size: %40 population size .....	28
Figure 3.2 Trials for maximum number of iteration. a) Iteration: 60, b) Iteration: 80, c) Iteration: 100, d) Iteration: 120, e) Iteration: 150 .....	30

Figure 3.3 Trials for population size. a) Population size: 100 individuals, b) Population size: 150 individuals, c) Population size: 200 individuals.....	32
Figure 3.4 Pareto front solutions for optimization framework .....	34
Figure 3.5 Change of geometry variables from min. PoD (Rep_1) to max. Range (Rep_80).....	37
Figure 3.6 3D view of “Rep_50” geometry .....	38
Figure 3.7 RCS signature of Rep_50 in dBm .....	39
Figure A.1 Three-variable, ten-point Latin hypercube sampling plan shown in three dimensions (top left), along with its two-dimensional projections [39]. .....	51
Figure B.1 Validation of MOPSO algorithm. a) MOPSO results for ZDT1 test function, b) true Pareto front for ZDT1 test function [29], c) MOPSO results for MOP2 test function, d) true Pareto front for MOP2 test function [29].....	54

## LIST OF SYMBOLS

$\alpha_m$	Coefficient of the expansion
$\beta_m$	Basis function
$K_m$	Number of factors in the $m$ -th basis function
$x_{v(k,m)}$	$v$ -th variable
$t_{k,m}$	Knot location on each of the corresponding variables
$\Phi_q$	Scalar-valued criterion function
$J_j$	Number of pairs of points in $X$ separated by the distance $d_j$
$X$	Sampling plan
$d_j$	List of the unique values of distances between all possible pairs of points in a sampling plan $X$
$RMSE$	Root Mean Square Error
$X_{real}$	Real values of $X$
$X_{metamodel}$	Estimated values of $X$
$R$	Range of aircraft
$V_\infty$	Constant flight velocity
$c$	Specific fuel consumption
$L/D$	Lift-to-drag ratio
$W_0/W_1$	Fuel weight fraction
$N_{RCS}$	Number of points that RCS value of greater than $0.1\text{m}^2$
$N_{total}$	Total number of points
$POD$	Possibility of detection
$S_{wg}$	Gross wing area
$b$	Wing span
$W_0$	Max. take-off weight
$W_e$	Empty weight
$W_{sys}$	Systems weight

$W_{engine}$	Engine weight
$n_{ult}$	Ultimate load factor
$\Lambda_{1/2}$	Half-span wing sweep
$(t/c)_{avg}$	Average wing thickness to chord ratio
$\lambda$	Wing taper ratio
$C_4$	System factor value
$T_{required}$	Required Thrust

## LIST OF ABBREVIATIONS

CFD	Computational Fluid Dynamics
DLR	Deutsches Zentrum für Luft- und Raumfahrt e.V.
DOE	Design of Experiment
GA	Genetic Algorithm
MARS	Multivariate Adaptive Regression Splines
MDO	Multidisciplinary Design Optimization
MOPSO	Multi-Objective Particle Swarm Optimization
MTOW	Maximum Take-Off Weight
NACA	National Advisory Committee for Aeronautics
NASA	Optimization Library
PoD	Possibility of Detection
RANS	Reynolds Averaged Navier Stokes
RCS	Radar Cross Section
RMSE	Root Mean Square Error
SAM	Surface to Air Missiles
SU2	Stanford University Unstructured
UCAV	Unmanned Combat Aerial Vehicle
VLM	Vortex Lattice Method

## CHAPTER 1

### INTRODUCTION

#### 1.1 Description of Unmanned Combat Aerial Vehicles (UCAV)

Unmanned Aerial Vehicles (UAVs) are becoming key players in modern combats scenarios. They are used in many missions including search and rescue, reconnaissance and even combat missions. To complete the successfully combat missions, some specifications, such as stealthiness, payload capacity and maneuverability, comes into picture. One of the main requirement in UCAV's design is stealthy, which means low observability of the aircraft for radars. The advantages of low observable aircraft is that the aircraft can fly deeper into enemy territory and will not be detected until it is very close to its target [1]. Although the low observable design increases the survivability of the aircraft, this creates a challenge in aerodynamics and performance of the aircraft. Therefore, the design of UCAV must be conducted as an optimization problem with many design requirements in multidiscipline.

There are many examples of UCAVs which has been designed and flied. Some of the example UCAVs are illustrated in Figure 1.1. While the tailless configurations are the common feature of design configurations, the planform shapes of the UCAVs differ with each other.



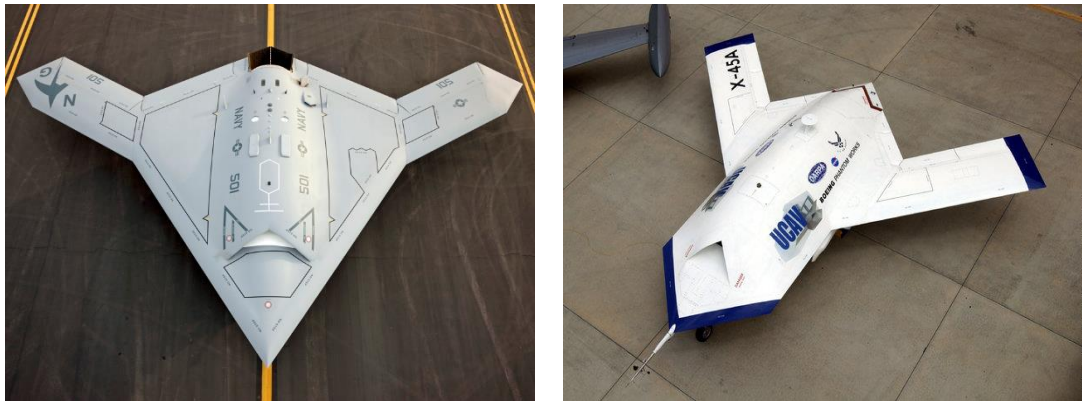


Figure 1.1 Example of UCAVs in the world. (Left upper: BAE Systems Taranis [2], Right upper: Dassault nEUROn[3], Left lower: Northrop Grumman X-47B[4], Right lower: Boeing X-45A[5])

UCAVs are designed to use in concept of operation (CONOPS) such as SEAD (Suppression of Enemy Air Defence), DEAD (Destruction of Enemy Air Defence), CAS (Close Air Support) and reconnaissance missions. The illustration of a typical SEAD/DEAD mission are given in Figure 1.2. For the conceptual design the requirements of each mission leg must be identified to be input for conceptual design. In Figure 1.3, a similar UCAV design mission given in Ref [1] with defined mission requirements. In this mission, the aircraft climbs to 11 km altitude and cruise with 0.8 Mach speed. The aircraft reaches its maximum speed of 0.9 Mach at dash to target. In here, a long cruise range is a significant requirement to maximize the mission range of the aircraft. Also, the aircraft must be low observable to SAM radars showed in Figure 1.2. Therefore, low observability and long cruise range will be the main requirements for the conceptual design of the UCAVs in this study.

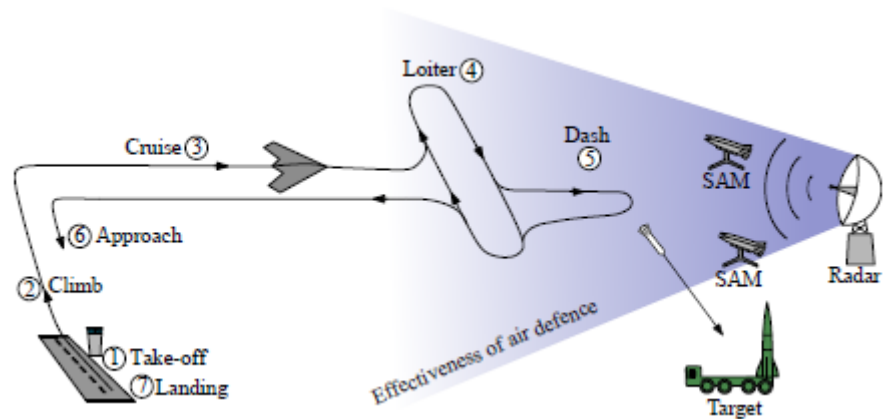


Figure 1.2 SEAD/DEAD mission [1]

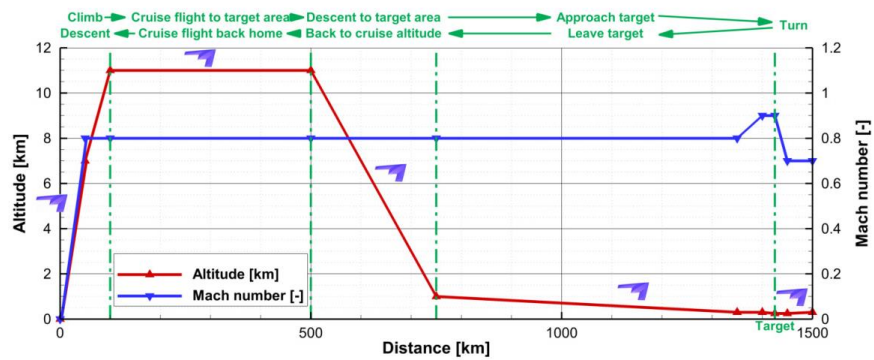


Figure 1.3 UCAV Design mission [6]

## 1.2 Literature Review

In Ref [6], multidisciplinary design for an agile and highly swept aircraft configuration is studied. The aircraft configuration is based on SACCON shape, for which the design features was carried out in a common effort within NATO STO/AVT-161 task group [7]. The SACCON configuration was sized to meet the mission requirements given in Figure 1.3. Moreover, comparison of the aerodynamic characteristics of the SACCON configuration predicted by low- and high-fidelity aerodynamic methods were studied. As a result, it can be stated that the coefficients from simple aerodynamic methods can be sufficient as long as the angles of attack are kept low.

Ref [8] presented a conceptual design on SACCON 1303 geometry while using conceptual design and optimization program. The sensitivity of vehicle weight to various criteria including the aerodynamic performance of the wing is investigated.

In Ref [9], multi-objective multidisciplinary design optimization of UCAV was studied according to aerodynamics, stealth and structures. Surrogate modeling (also called as meta-modeling) technique was used to construct a simplified mathematical approximation of computationally expensive simulations. The optimization was run for minimum weight and minimum drag with the constraint of low radar cross section signature.

Ref [10] focused on developing a methodology for carrying out conceptual sizing of a UCAV based on initial sizing, constraint analyses and refined sizing. The SACCON 1303 geometry was used as a baseline configuration. Multi-objective optimization was conducted with assessment of aerodynamic and stealthy disciplines. The trade-off between take-off length and wing span was obtained as results of study.

Ref [1] studied to develop novel design methodology that aiming to minimize drag at cruise while ensuring the leading edge flow remains attached at take-off phase. The SACCON 1303 geometry was used as a baseline configuration. In this optimization problem, the multiple objective were handled with assessment of only aerodynamics.

In Ref [11], multidisciplinary design optimization of UCAV was studied with variable fidelity modeling method. It was aim to create a design framework for UCAV and minimize the take-off gross weight. Both low fidelity and high fidelity tools were used in design framework to size the aircraft. For high fidelity aerodynamic analysis, 20 cases were analyzed by high fidelity CFD code and surrogate model was constructed from these results. Genetic algorithm was selected to seek global optimum point for this problem.

Ref [12] detailed a software tool for conceptual design of blended wing body aircraft with a multidisciplinary approach. The tool consists of four main modules,

which are an aerodynamic model, a model of the wing box structure, a model for the cabin, and a model for the fuel tank. The geometry of model was represented with 30 design variables. A gradient-based optimization routine was employed to find a combination of the design variables that satisfies all constraints while optimizing for cruise range at constant maximum take-off weight.

Ref [13] presented a research on aircraft conceptual design process by the application of multidisciplinary optimization (MDO). Both gradient based optimization methods and evolutionary algorithm methods were compared in the optimization of four different aircraft concepts. Six variables (Thrust to weight ratio or power loading, wing loading, aspect ratio, taper ratio, sweep angle, airfoil max. thickness to chord ratio) were considered for aircraft conceptual design optimization. This author identified these variables as the most important optimization parameters in conceptual design. The key conclusion of study is that aircraft conceptual design can be improved by the proper application of such MDO methods.

Ref [14] developed a multidisciplinary design optimization framework applied on UAV design. Five principle engineering disciplines, such as the geometric design, the aerodynamics, the antenna analysis, the radar cross section signature and the mission simulation, were evaluated related to aircraft design. Meta-model techniques were used for computationally expensive simulation and optimization process were handled with Multi-Objective Genetic Algorithm (MOGA-II).

Ref [15] aimed to develop a module for aerodynamic analysis which is one of the submodule of MDO framework for conceptual aircraft design. High order panel code, PANAIR, was used within the framework. This authors mainly intended to construct a MDO framework consisted of aerodynamics, stability and control, structure and basic aircraft systems modules. As a test case, the design of a UCAV was used and gradient (fmincon) and non-gradient based (Complex and GA) optimization methods were used to find minimum maximum take-off weight (MTOW) required to fulfil the mission. As a result of this study, it was understood that GA was the best optimization methods to find minimum MTOW in this scenario

and optimized configuration was very similar to competitor UCAVS, such as Boeing X-45C and Northrop Grumman X-47B.

### **1.3 Aim of this study**

When literature review is considered, it is clearly seen that conceptual design processes need to be performed by a multidisciplinary approach and optimization. Aerodynamics, structures, weight estimation, flight performance, observability and a multitude of different disciplines must be evaluated during the conceptual design stage. Furthermore, the requirements of low observability and long cruise range, will definitely drive the design of aircraft. Hence, the aim of this study is to create a multi-disciplinary design framework with multi-objective optimization.

The present work is intended to be a multi-disciplinary design optimization process consisting of sub modules, such as aerodynamics, weight estimation, radar cross section signature and optimization. It is easy to increase the capability and fidelity of the framework with the addition of new modules to the present framework or replace the existing modules with new ones.

### **1.4 Outline of the presented work**

The first chapter consists of a background and a description of UCAVs, literature review about multidisciplinary design of UCAVs and aim of this study.

The second chapter explains the development of optimization framework to design UCAVs. Firstly, general description of framework is presented. Then, each module of framework is described with details.

The third chapter provides results and discussion of study. The outputs of framework is evaluated in here.

In the last chapter, the conclusion of the study and possible future work are given.

## CHAPTER 2

### DEVELOPMENT OF OPTIMIZATION FRAMEWORK

This chapter is devoted to a brief explanation of the present regarding optimization framework which includes modules of aerodynamics, radar cross section, weight estimation and their optimization.

#### 2.1 General Description of Framework

General description of optimization framework is presented here. Framework consists of modules for generating the 3D geometry, analysis of each disciplines, performance calculations and their optimization. This framework structure allows changing and replacing the each module or adding new modules to use in another design problem later on. The scheme of optimization framework is presented in Figure 2.1.

To explain the general working scheme of the framework, at first, design variables are created for individual or population in the defined design space. Then, using with these design variables, the 3D geometry is generated for an input into the aerodynamic analysis, radar cross sectional analysis and to the weight estimation modules. The results of analysis are used for calculating performance (objective function) of individual or population. Optimization process continues iteratively until the convergence criterion met.

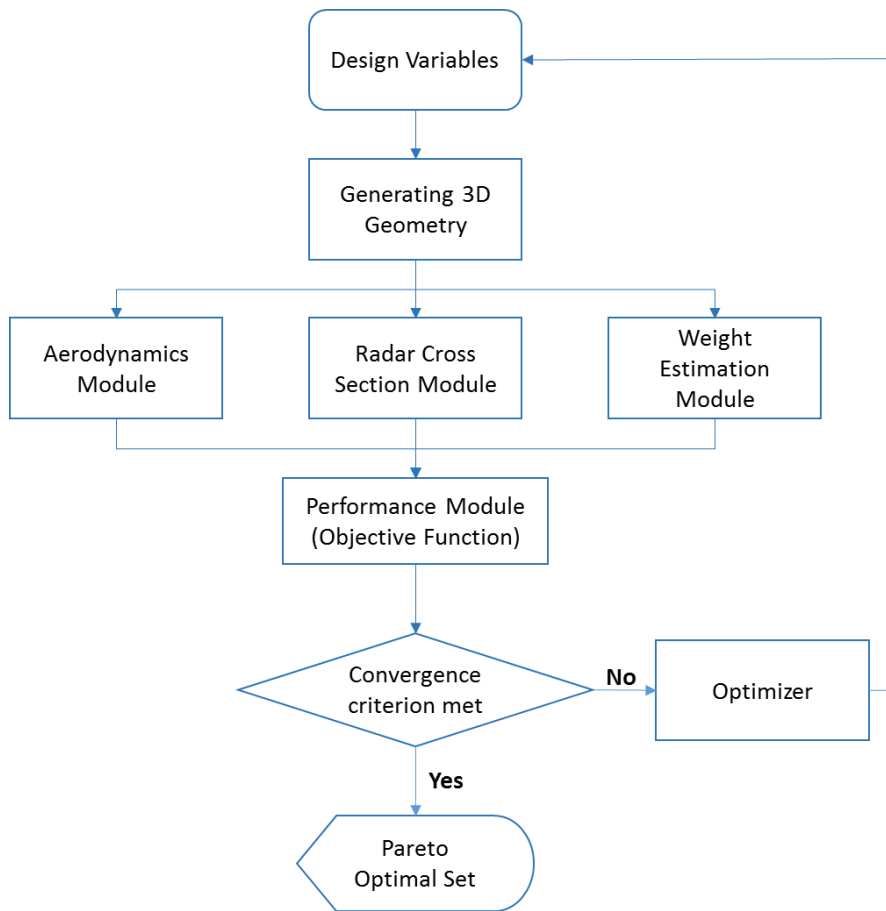


Figure 2.1 General scheme of optimization framework

Further details of the scheme of the framework will be discussed in the following sections. To define the design variables, the geometry of considered aircraft must be parameterized. In this study, the aircraft is a UCAV and SACCON 1303 geometry given in Figure 2.2 and is chosen as a conceptual geometry. The reason of choosing this geometry is that stealth requirements drive the aircraft design to flying wing concept. The parameterization of SACCON 1303 geometry is shown in Figure 2.3. To shorten the computational time and avoid unfeasible geometries, some assumptions and constraints are considered. Thus, design variables are created and are shown in Table 2.1.

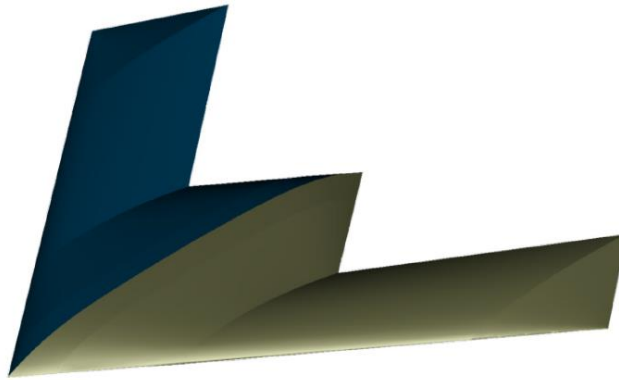


Figure 2.2 SACCON 1303 geometry [6]

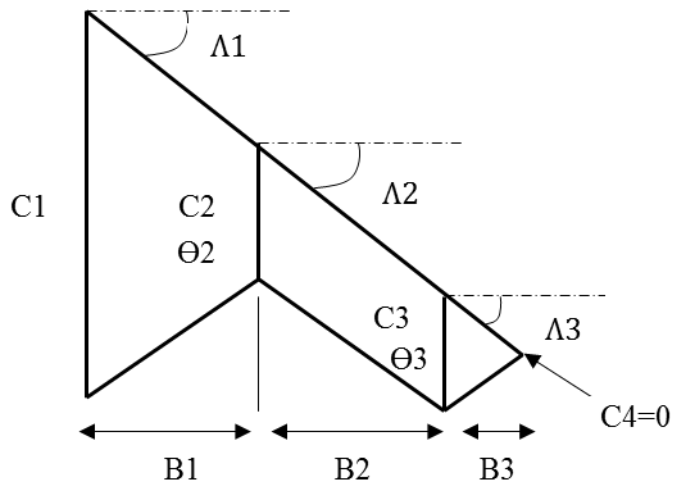


Figure 2.3 The parameterization of SACCON 1303 geometry

Table 2.1 Design variables and assumptions

Geometry Parameters	Assumptions/Constraints	Design Variables
Chord lengths: $C1, C2, C3, C4$ Span lengths: $B1, B2, B3$ Sweep Angles: $\Lambda1, \Lambda2, \Lambda3$ Twist Angles: $\Theta2, \Theta3$	$C4 = 0$ ; $\Lambda = \Lambda1 = \Lambda2 = \Lambda3$ ; $C2 > C3$ Airfoils: $C1$ : NACA 64012 $C2$ & $C3$ : NACA 64008	Chords: $C1, C2, C3$ Spans: $B1, B2, B3$ Sweep Angles: $\Lambda$ Twist Angles: $\Theta2, \Theta3$

Now, design space must be defined for chosen design variables. In this study, DLR F-19/SACCON configuration is considered as a starting point [6]. Therefore, the lower and upper bounds of the design space are sized according to DLR F-19/SACCON configuration. The lower and upper bounds that will be searched to get Pareto results are given in Table 2.2.

Table 2.2 The lower and upper bounds of design space

Design Variable	Lower Bound	Upper Bound
Span Length (B1)	2	3
Span Length (B2)	2.5	3.5
Span Length (B3)	0.5	1.5
Chord Length (C1)	9	11
Chord Length (C2)	5	7
Chord Length (C3)	3	6
Twist Angle ( $\Theta_2$ )	-5	5
Twist Angle ( $\Theta_3$ )	-5	5
Leading Edge Sweep ( $\Lambda$ )	40	60

Three-dimensional geometry is created with OPENVSP software, which is published by NASA. OpenVSP is a parametric aircraft geometry tool which allows the user to create 3D model of an aircraft defined by common engineering parameters. The software is very easy to use, user friendly and can also be run in dos-system with script. With this capability, OPENVSP is a perfect sketch tool for optimization process.

In Aerodynamics module, lift-to-drag ratio of the aircraft is calculated at level flight for chosen mission altitude and velocity. For calculation of lift and drag, Aerodynamics solver is selected as compressible Euler Solver. The reason of using compressible Euler Solver instead of RANS Solver is less need of computational

cost. This choice reduce both the computational cost of solution and complexity of automatic mesh generation. The disadvantages of Euler solver is its lack of viscosity effect. However, the FRICTION code, which uses the component build-up method, is used to incorporate the viscous effects on the drag in aerodynamic calculations [16]. Further details and process about aerodynamics module is explained in Section 2.2.

In RCS module, radar cross section signature of the aircraft is calculated. Radar cross section (RCS) is a measure of the power scattered in a given direction when a target is illuminated by an incident wave, normalized to the power density of the incident field [17]. To calculate RCS signature, POFACETS [18], which is an implementation of the physical optics approximation for predicting the RCS of complex objects, is employed. In this stage, monostatic radars, where the radar and the receiver are in the same place, are chosen as threats. When the SAM radars specified in the task description are examined, it is seen that the frequency range is generally in the S band frequency range. Therefore, the frequency was selected as 3 GHz in the radar trace analysis. Since the radar's longitudinal elevation is small at the distance that the aircraft enters the radar range, the longitudinal elevation is considered as zero. Further details and process about RCS module is explained in Section 2.3.

Weight Estimation module use empirical/statistical formulas to estimate the maximum take-off weight. Maximum take-off weight of aircraft consists of empty weight, payload weight, fuel weight. Structural weight of vehicle, systems weights (avionics, landing gears, etc.) and engine weight are estimated as subparts of empty weight. Payload weight is fixed from mission requirements. Fuel weight is kept as a fixed ratio according to maximum take-off weight. Further details and process about weight estimation module is explained in Section 2.4.

In aerodynamics and RCS modules, meta-modeling techniques are used to accelerate the optimization process. Multivariate Adaptive Regression Splines (MARS) method is used as meta-modeling technique. Detailed derivation of the method can be found in Appendix A.

There are two objectives as performance parameters for UCAV design: Range and Possibility of Detection. Range of the air vehicle is calculated using the Brequet range equation [19].

$$R = \frac{V_{\infty} L}{c D} \ln \frac{W_0}{W_1} \quad (2.1)$$

Where,  $V_{\infty}$  is constant flight velocity,  $c$  is specific fuel consumption,  $L/D$  is lift-to-drag ratio and  $W_0/W_1$  is fuel weight fraction.

Possibility of detection is the ratio between the number of points that RCS value of greater than  $0.1\text{m}^2$  and total number of points.

$$PoD = \frac{N_{RCS}}{N_{total}} \quad (2.2)$$

Where  $N_{RCS}$  is the number of points where RCS value is greater than  $0.1\text{m}^2$  and  $N_{total}$  is the total number of points. As an example, RCS signature of example UCAV geometry are given in both polar and linear plots.

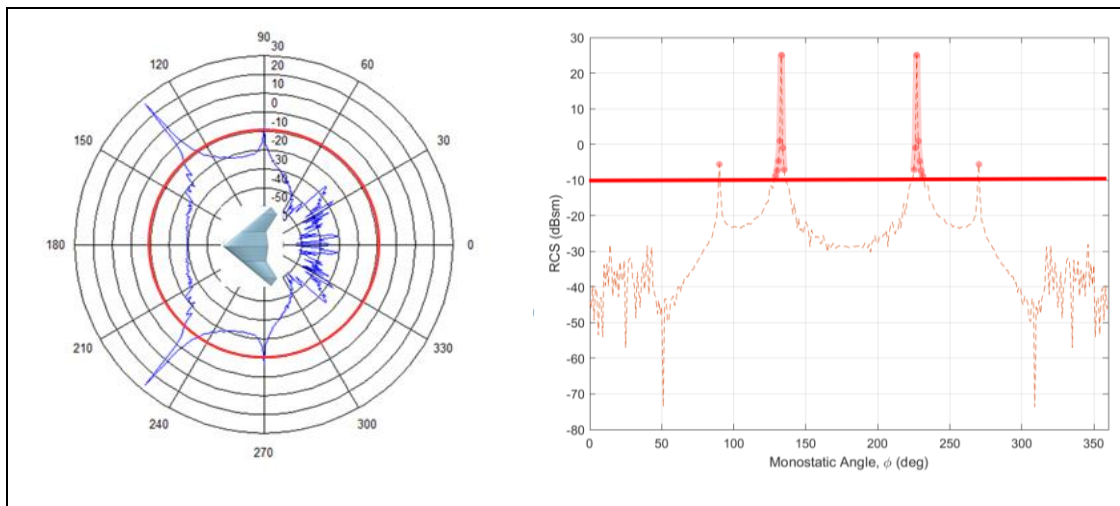


Figure 2.4 RCS signature of example UCAV in both polar (left) and linear (right) plots

With these objectives, it is aimed to achieve to UCAV geometries that are changed between maximum range and minimum possibility of detection.

The methodology that incorporates the multi-objective multi-disciplinary design optimization is driven by Multi-Objective Particle Swarm Optimization (MOPSO) function which is based on the paper of Coello Coello et al [20]. Since every multi-objective optimization aims to get Pareto optimal set, it is obtained by performing the Pareto Envelope and grid making technology in this framework. Further details and processes about Optimization module and MOPSO method are explained in Section 2.5.

## **2.2 Aerodynamic Module**

Aerodynamic module performs aerodynamic analysis for given individual. The output of the aerodynamic module is the lift-to-drag ratio of the aircraft at level flight for chosen mission altitude and velocity. To perform aerodynamic analysis, there are many studies in the literature, which use low fidelity methods, like Vortex Lattice Method (VLM), or high fidelity methods, like Computational Fluid Dynamics (CFD) as a solver. Solver selection defines the fidelity of analysis. As fidelity increases, computational time increases as well. The meta-modeling techniques are used to overcome this dilemma. The comparison and evaluation of analysis methods and the methodology used in this study are explained in this section.

VLM is a low fidelity method which is used in conceptual design phases because of the low computational time. Therefore, more points can be covered in specific design space in a certain time with VLM solver compared to high fidelity tools. The disadvantage of VLM is that it neglects the viscous effects, body-interaction effects and compressibility effects. [21]. Therefore, Prandtl-Gauert compressibility correction is used in most VLM solver to reflect the compressibility effects in solution. The viscous effects can be included as a parasite drag with external calculations. The FRICTION code, which use drag build-up method, can be

used to calculate parasite drag of aerial vehicles [10], [16]. In the study of Gur and et.al, drag calculation with FRICTION code for subsonic wing and transonic wing is validated with experimental data and can be used in the conceptual design phase [16].

Unlike VLM solver, CFD is a high fidelity tool and needs high computational effort to solve a problem. RANS and Euler methods are options for CFD solution. RANS solutions consist of viscosity, compressibility and turbulence effects. Therefore, computational effort increases when RANS solution is preferred. However, Euler solution consists only compressibility effects but it is computationally faster than RANS solutions. When it is compared with VLM methods, compressibility effects are modelled in the Euler equation not modelled by corrections. Therefore, compressibility effects in Euler solutions are more feasible than VLM solutions.

After the evaluation of aerodynamic solvers, it is decided to use compressible Euler method for aerodynamic analysis. Viscous effects are included as a parasite drag with using component build-up method (FRICTION code). The methodology used in this study is illustrated in below scheme.

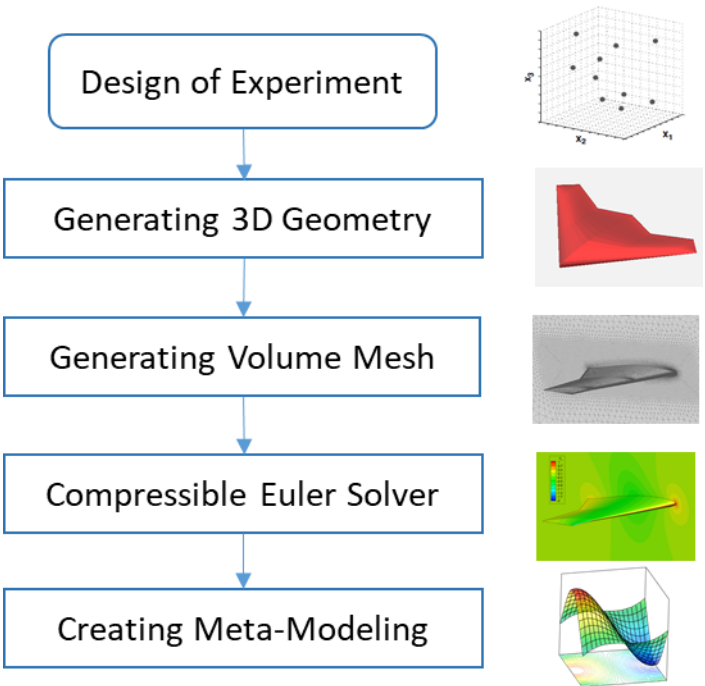


Figure 2.5 Methodology of creating aerodynamic meta-model

Design of experiment (DOE) is created using Optimized Latin Hypercubes method. DOE consists of uniformly distributed 100 sample points. For all sample points, 3D geometries are created in “.iges” format with OPENVSP and then volume meshes are generated with using unstructured mesh in Pointwise, mesh generator tool. Pointwise is a powerful software that capable of generating many types of meshes for CFD. Pointwise also includes scripting language that can be used to write macros and templates for automating all the meshing process. In Figure 2.6, the overview of the mesh density generated in Pointwise can be seen.

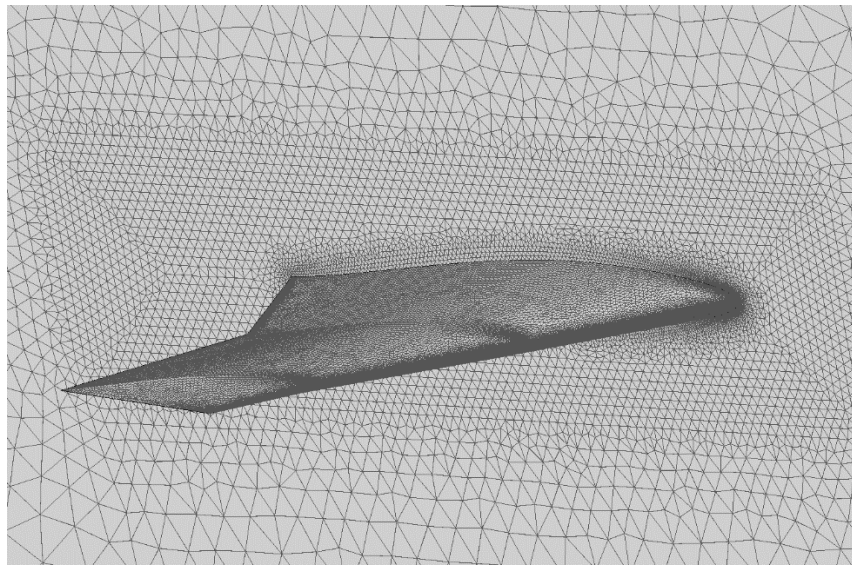


Figure 2.6. Overview of mesh density

Although there are many commercial CFD solvers, like ANSYS Fluent, CFD++, Star CCM+ and open-source CFD solvers, like SU2 and OpenFOAM, open-source SU2 is preferred as a flow solver in this study.

SU2 is an open source, computational analysis tool which is collection of software tools written in C++ for performing Partial Differential Equation (PDE) analysis and solving PDE-constrained optimization problems. The toolset is designed with Computational Fluid Dynamics (CFD). SU2 is under active development by Aerospace Design Lab (ADL) of Stanford University and is released under an open-source license.

Flight conditions for CFD simulations are defined in cruise mission profile as flying with 0.8 Mach velocity and at 11 km altitude. Although the in the depth analysis of CFD solutions is not in the scope of the thesis, a few details are given below:

- The solution domain is created sufficiently large to satisfy the freestream conditions.
- High-quality mesh of 6 million elements was generated. Edge sizing was used in the critical regions.
- To decrease the computational time, compressible Euler equations was used instead of RANS equation.
- For each sample in DOE, CFD simulations are done in five different angles of attack at defined steady state flight conditions.

As an example of CFD simulation, the pressure distribution at 1° angle of attack is illustrated in Figure 2.7.

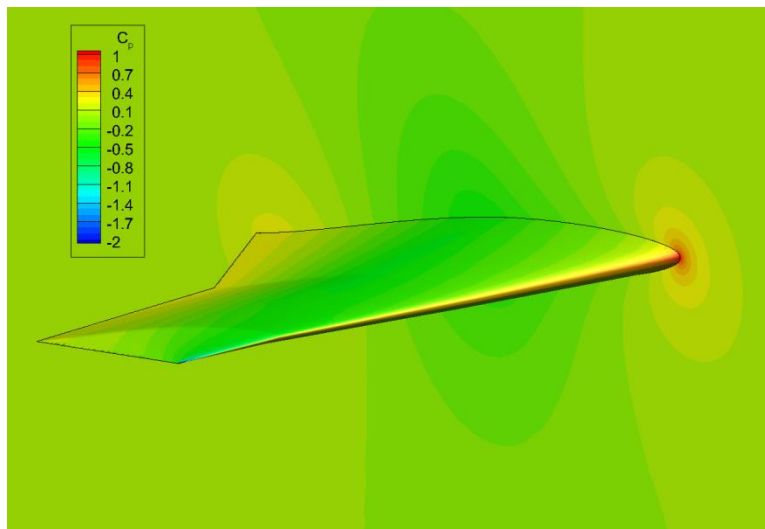


Figure 2.7 Pressure distribution for one of the sample UCAV geometry

After CFD solutions, design lift-to-drag ratios for each sample are calculated. In here, the design lift-to-drag ratio is the ratio between lift and drag values at angle of attack, where lift equals the weight of the aerial vehicle in required cruise speed

and altitude. Aerial vehicle's weight is calculated by using the weight estimation module for all samples.

Now, we have 100 sample points and their aerodynamic results as a design lift-to-drag ratio. Therefore, the meta-model of aerodynamics is generated using MARS meta-modeling technique. To check the accuracy of the metamodel, the metamodel results and CFD results are compared with using another sample set. Generated aerodynamic meta-model is a good model with %6.12 Normalized RMSE value. As a result, we have the aerodynamic module that has fidelity of compressible Euler solution and computation speed of running basic Matlab function.

### **2.3 Radar Cross Section (RCS) Module**

Stealthiness is a major necessity for successfully completion of the mission. UCAV must fly deeper into the enemy territory without detected to any radar. A radar can briefly explained that a device transmits an electromagnetic wave and detects objects by virtue of the energy scattered from them in the direction of the receiver [17]. Therefore, UCAVs have to be designed so that small portion of the energy from the illuminating radar is scattered in tactical sectors, and most of the energy is scattered in directions considered to be safe [22].

Stealth concept is not only related with low RCS. All types of signatures must be considered, such as thermal infrared, visibility to the human eye, and the acoustic signature. However, low RCS is an important aspects because most modern military forces are in possession of radar systems [23]. Therefore, RCS signature analyses must be included as another discipline in the conceptual design phase. There are many numerical methods to analyze RCS in literature, such as Finite Difference-Time Domain Technique (FD-TD), Method of Moments (MOM), Geometrical Optics (GO), Physical Optics (PO), Geometrical Theory of Diffraction, Physical Theory of Diffraction (PTD) [24].

In the scope of this thesis, a Matlab-based code POFACETS, which uses a Physical Optics method, is used to obtain RCS signature. POFACETS program is an inexpensive, easy to use, RCS prediction software tool that is capable of predicting

RCS rapidly and accurately within small amounts of time for arbitrary three-dimensional geometries. Target model to be analyzed is defined by using of triangular facets as in Figure 2.8. Physical Optics method is used to calculate current on illuminated facets. Current is set to zero in non-illuminated facets. Radiation integrals and Taylor series are used to compute the scattered field from each facet. Total scattered field is sum of the fields from each facet. The effects of diffraction, multiple reflections, and shadowing, surface waves are not included in these calculations [18]. RCS is computed as:

$$\sigma = 4\pi \frac{|\vec{E}_s|^2}{|\vec{E}_i|^2} \quad (2.3)$$

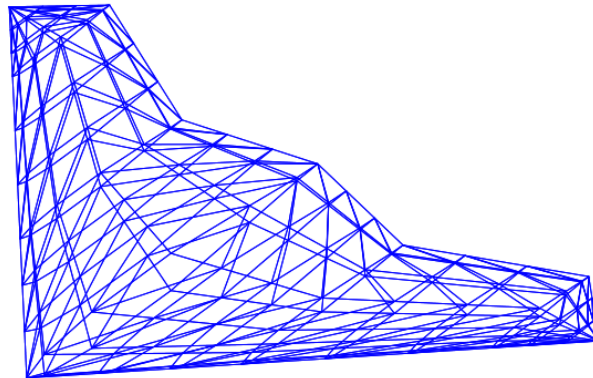


Figure 2.8 Target model defined by using of triangular facets

RCS calculations become computationally expensive when they are considered in optimization iteration. Therefore, meta-modeling technique is applied in RCS analysis and RCS module is represented as meta-model. The meta-modeling process of RCS analysis are illustrated in Figure 2.9.

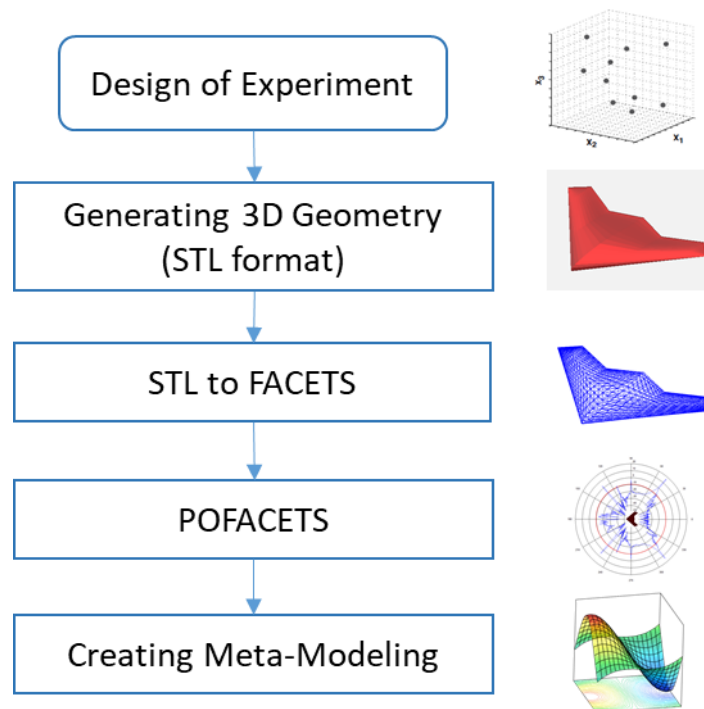


Figure 2.9 The meta-modeling process of RCS analysis

Design of experiment (DOE) is created using Optimized Latin Hypercubes method. DOE consists of uniformly distributed 100 sample points. For all sample points, 3D geometries are created in “.stl” format with OPENVSP. Before the calculation of RCS signature, 3D geometries in “.stl” format are converted to facets. For the calculation of RCS signature, threats must be identified first. In this study, monostatic radars, where radar and receiver are in the same place, are chosen as threats. SAM radars can be example of monostatic radars and their frequency range is generally in the S band frequency range. Therefore, the frequency was selected as 3 GHz in the radar trace analysis. Since the radar's longitudinal elevation is small at the distance that the aircraft enters the radar range, the longitudinal elevation is considered as zero. Therefore, the calculation of monostatic RCS are executed in xy plane of body frame. The polar plot of RCS signature is given in Figure 2.10 as an example. As RCS performance criteria, the possibility of detection is defined. Possibility of detection (PoD) is the ratio between number of points that RCS value of greater than  $0.1\text{m}^2$  (-10 dbm) and total number of points.

The meta-model of RCS is generated using MARS meta-modeling technique with 100 sample points and their PoD results as a design criteria. To check the accuracy of the metamodel, the metamodel results and CFD results are compared with using another sample set. Generated RCS meta-model is a good model with %10.9 Normalized RMSE value. As a result, we have the RCS module that has fidelity of POFACETS and computation speed of running basic Matlab function.

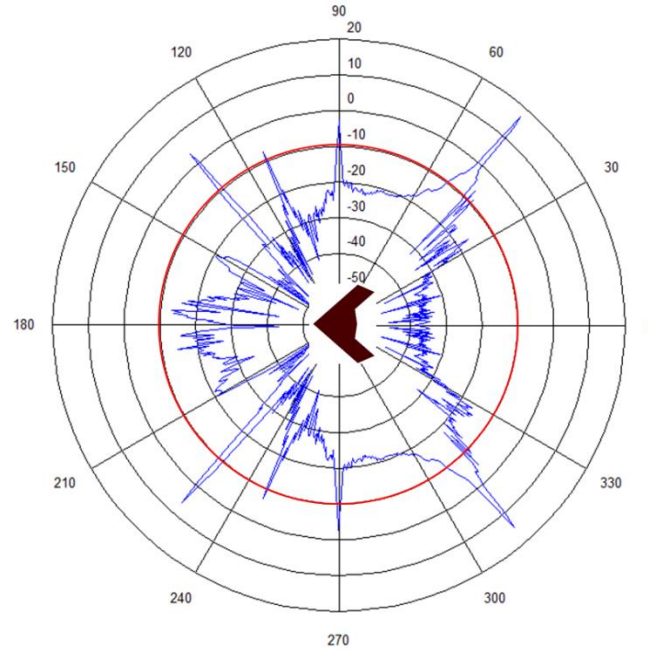


Figure 2.10 The polar plot of RCS signature

## 2.4 Weight Estimation Module

Weight estimation module is used to estimate maximum take-off weight of the aerial vehicle. Maximum take-off weight is the total of empty weight, fuel weight and payload weight. Empty weight comprises structural weight of vehicle, systems weights (avionics, landing gears, etc.) and engine weight. Fuel weight is assumed as %30 of the maximum take-off weight. Payload weight is total weight of the munitions given in the mission requirements.

$$W_0 = W_{empty} + W_{fuel} + W_{payload} \quad (2.4)$$

For estimation of empty weight, each subpart weight is calculated with different approaches. The structural weight is estimated with using Shevel's empirical formula [25]. The UCAV geometry consists of only wing structure. Therefore, Shevel's wing structural weight estimation is used. Wing structural weight is estimated in terms of ultimate load factor, wing dimensions, and max. take-off gross weight, max. zero fuel weight. This formula is illustrated in Equation 2.10. For system weight estimation, Howe's empirical formula is used [26]. This formula can be seen in Equation 2.11. Systems weight is determined by system factor value ( $C_4$ ) times max. take-off weight. System factor values is changing depend on the type of aircraft and is selected as subsonic bombers type of aircraft ( $C_4 = 0.12$ ). Engine weight estimation is performed with statistical formula, generated from performance database of 150 engine. The relation between thrust and engine weight can be seen in the Figure 2.11. The thrust-to-weight ratio of aircraft is determined as 0.35 respect to similar aircrafts.

$$W_{wing} = S_{wg} \left( \frac{1.6574 n_{ult} b^3 \sqrt{W_0 W_e} (1 + 2\lambda)}{\left(\frac{t}{c}\right)_{avg} \cos^2(\Lambda_{1/2}) S_{wg}^2 (1 + \lambda)} \times 10^{-6} + 4.0569 \right) \quad (2.5)$$

Where the inputs are gross wing area ( $S_{wg}$ , sqf.), wing span ( $b$ , ft), max. take-off weight ( $W_0$ , lb), empty weight ( $W_e$ , lb), ultimate load factor ( $n_{ult}$ ), half-span wing sweep ( $\Lambda_{1/2}$ ), average wing thickness to chord ratio ( $(t/c)_{avg}$ ), wing taper ratio ( $\lambda$ ).

$$W_{sys} = C_4 W_0 \quad (2.6)$$

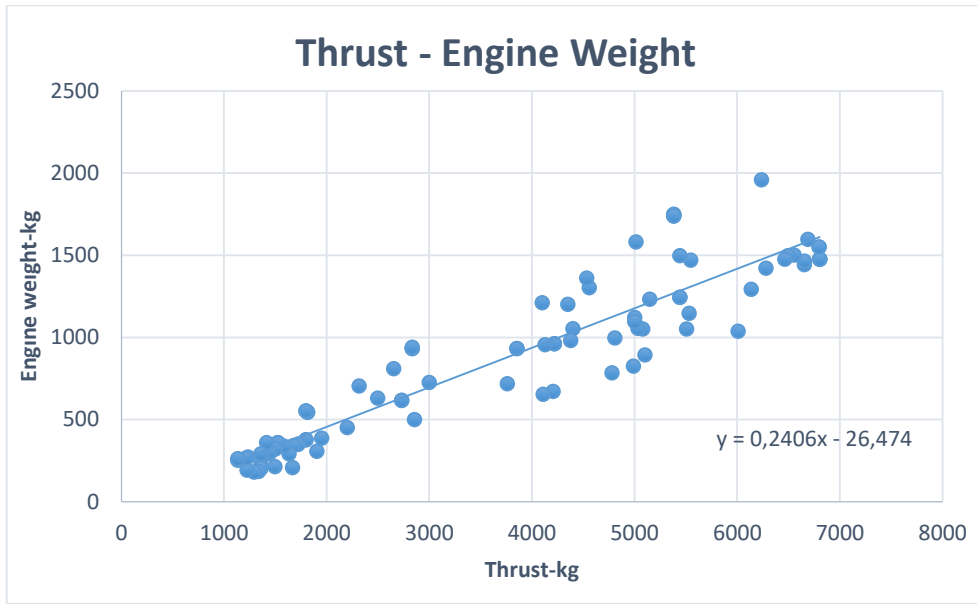


Figure 2.11 Thrust vs. Engine weight relationship

$$W_{engine} = 0.2406T_{required} - 26.474 \quad (2.7)$$

In Walker's thesis, weight estimation techniques and methods are evaluated. The accuracy of Shevel's wing weight estimation and Howe's weight estimation is considered very good accuracy rating with 0% exclusion rate for most of the validation aircrafts [27]. For similar UCAVs, weight estimation is performed. Actual and estimated weights can be seen in Table 2.3. Although weight estimation for X-47A and X-47B are so close to actual values, the error of calculated weight for X-45A and Neuron aircrafts are significant. Nevertheless, the methods used in here are low fidelity empirical methods and this results are acceptable for this stage of study.

Table 2.3 Actual and estimated weights

A/C	ACTUAL		CALCULATED		ERROR	
	Empty Weight, kg	MTOW, kg	Empty Weight, kg	MTOW, kg	Empty Weight, kg	MTOW, kg
X-45A	3630	5530	2408	4308	-34%	-22%
X-47A	1740	2678	1735	2673	0%	0%
X-47B	6350	20215	6377	20242	0%	0%
Neuron	4900	7000	3437	5537	-30%	-21%

## 2.5 Optimization Module

In the scope of the thesis, there are two design objectives to be optimized; range and possibility of detection. To solve this design problem, a number of disciplines are considered. Therefore, this problem is called as a multi-objective multi-disciplinary design optimization problem. Multi-objective optimization aims to get the Pareto optimal set, which is a set of non-dominated solutions, being chosen as optimal [28]. Pareto optimal set is also called as Pareto front. The non-dominated solutions are a set of all the solutions that are not dominated by any member of the solution set.

Optimization methods are generally divided to as gradient-based and gradient-free. Among gradient-based methods adjoint method, automatic differentiation method and complex step derivative method can be considered; among gradient-free methods evolutionary methods can be considered. Each method has its strength and weakness, the choice is problem dependent. Evolutionary algorithms seem to be particularly suited to multi-objective problems due to their ability to synchronously search for multiple Pareto optimal solutions and perform better global exploration of the search space [29]. There are several different evolutionary algorithms, like Non-dominated Sorting Genetic Algorithm (NSGA), Strength Pareto Evolutionary Algorithm (SPEA), Pareto Archived Evolution Strategy (PAES), Micro-Genetic Algorithm (Micro-GA) and Multi-Objective Particle Swarm Optimization (MOPSO). When MOPSO, SPEA, NSGA and PAES methods are compared according to their performances to find Pareto front, MOPSO is the only algorithm that is able to cover the full Pareto front [30], [31]. In this study, MOPSO algorithm is chosen as an optimization method.



Figure 2.12 Swarm behavior of birds [32]

Multi-Objective Particle Swarm Optimization (MOPSO) was first introduced by Coello et al [20]. MOPSO is the adapted version of Single Objective Particle Swarm Optimization (PSO) method for multiple objective optimization. The idea of PSO is based on flocking behavior (of birds, fish, etc.), where the direction of movement of an individual is effected by the locations and movement of neighboring individuals (Figure 2.12). In PSO, a swarm of particles is moving in design space. Each particle maintains a local best position of its own trajectory, and a global best position from the neighborhood of the particle. In each generation, positions of all particles are updated by a velocity term, which is the weighted sum of three components: the inertia term equal to former velocity, distance to local best and distance to global best [31]. In MOPSO, particles share their information and move towards local and global bests just like in PSO. However, unlike PSO, Pareto-dominance relation defines the update of the local best. When new position dominates the former local best, it replaces the local best position. For global best selection, the algorithms usually maintain a set of non-dominating positions, also called as leaders archive or repository. To generate repository, Pareto Envelope and

hyper-grid techniques are used in MOPSO, similar to Pareto Envelope-based Selection Algorithm method [33]. This can be simply illustrated in Figure 2.13.

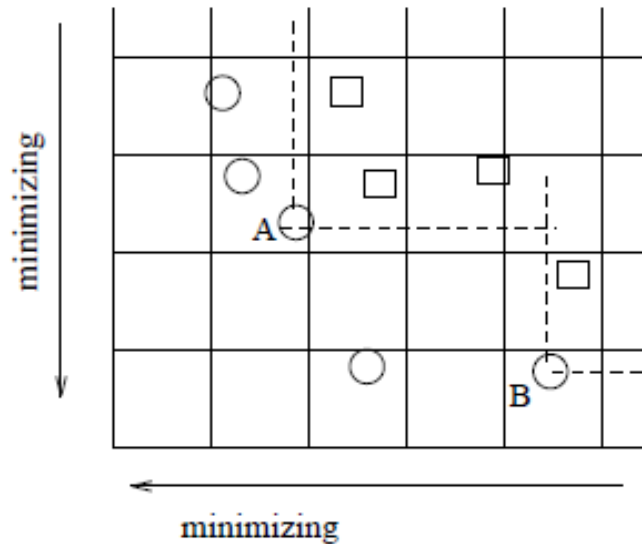


Figure 2.13 PESA's archive generation

The pseudocode of general MOPSO algorithm can be explained in Table 2.4 [34]. Firstly, swarm (or population), Leaders Archive (or Repository) are initialized. After initialization, some quality measure has to be calculated for all the leaders to select one leader for each particle of the swarm. In the main loop of algorithm, firstly, a new leader is selected and then, new positions of swarm are calculated. Mutation process can be applied as an option. After these steps, the particle is evaluated and its corresponding personal best solution "pbest" is updated. After each iteration, the set of leaders is updated and the quality measure is calculated again. When termination criteria is satisfied, the archive is returned as result of the search. The validation of this method with some test functions can be found in Appendix B part. As a results of validation, The MOPSO method achieves to find Pareto front results successfully for each test functions.

Table 2.4 The pseudocode of general MOPSO algorithm

<b>The pseudocode of general MOPSO algorithm</b>
1: initializeSwarm()
2: initializeLeadersArchive()
3: determineLeadersQuality()
4: generation = 0
5: <b>while</b> generation < maxGenerations <b>do</b>
6: <b>for</b> each particle <b>do</b>
7:         selectLeader()
8:         updatePosition()
9:         mutation()
10:         evaluation()
11:         updatePbest()
12: <b>end for</b>
13:     updateLeadersArchive()
14:     determineLeadersQuality()
15:     generation ++
16: <b>end while</b>
17: returnArchive()

To clarify the optimization problem, the optimization problem formulation with design variables are illustrated in Table 2.5.

Table 2.5 The optimization problem formulation

<i>Design Variables</i>	<i>Objective Functions</i>	<i>Constraints</i>
<i>Chords: C1, C2, C3</i>	Obj.1: <b>Minimize PoD</b>	$W_{fuel}/W_{total} = 0.30$
<i>Spans: B1, B2, B3</i>	(Possibility of Detection)	$T/W = 0.35$
<i>Sweep Angles: <math>\Lambda</math></i>	Obj.2: <b>Maximize Range</b>	$L/D @ L = W$
<i>Twist Angles: <math>\theta_2, \theta_3</math></i>		

The parameters of optimization methods must be defined to run the optimization. The population size of the swarm, the maximum number of iteration and the repository size will be defined in Chapter 3.

## CHAPTER 3

### RESULTS AND DISCUSSIONS

#### 3.1 Results

In Chapter 2, the multidisciplinary design optimization framework for UCAV conceptual design was developed. Methods and assumptions were explained with details for each discipline to be considered in this framework. Range and Possibility of Detection (PoD) were defined as design driven parameters. We are seeking Pareto front for maximum range and minimum PoD in defined design space.

Before the parameters of optimization methods were defined, the effect of parameters to Pareto set results was investigated. In Table 3.1, these parameters and their values are illustrated. The change of Pareto set for different configuration of parameters are observed.

Table 3.1 Optimization parameters

<i>Optimization parameters</i>	
<i>Population size of the swarm</i>	100, 150, 200
<i>Maximum number of iteration</i>	60, 80, 100, 120, 150
<i>Repository size</i>	%20, %30, %40 Population size of swarm

The repository size was tried for %20, %30 and %40 of population size of swarm. Other optimization parameters were fixed in order to understand effect of repository size to Pareto set. Population number was selected as 200 and maximum number of iteration was set as 150. As seen in Figure 3.1, when repository size equals %20 of population size, the members of repository are not enough to cover all Pareto front. When the repository size increases, Pareto front can be well covered.

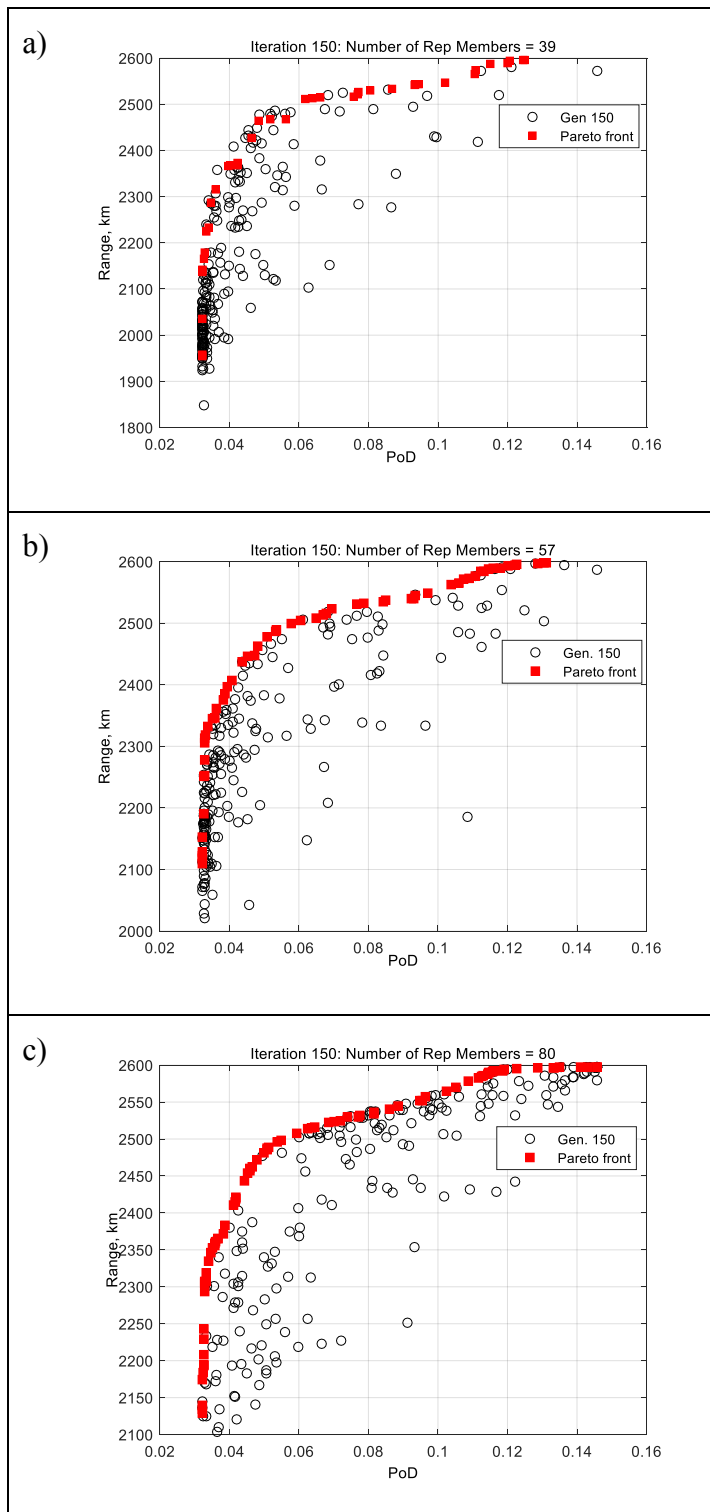
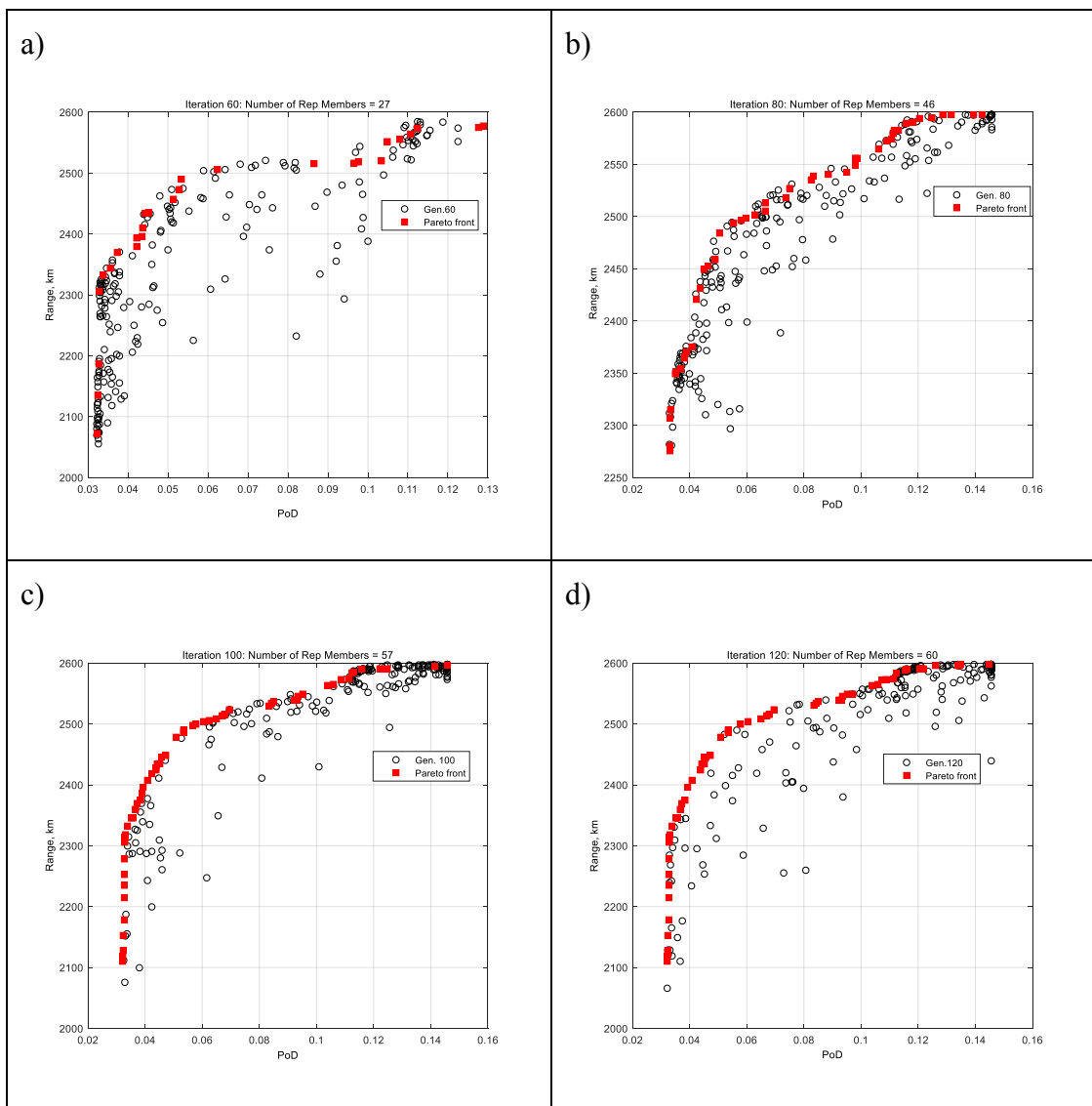


Figure 3.1 Trials for repository size. a) Repository size: %20 population size, b) Repository size: %30 population size, c) Repository size: %40 population size

The maximum number of iteration is another parameter to investigate. The investigation was carried out for 60, 80, 100, 120 and 150 maximum number of iteration when the population number and repository size were set fixed respectively as 200 and 60 members (%30 of the population size). The effect of this parameter to Pareto front results can be shown in Figure 3.2. At 60<sup>th</sup> and 80<sup>th</sup> iteration, it is seen that repository members cannot cover the Pareto front. However, at 100<sup>th</sup> iteration and after, Pareto front is clearly seen.



e)

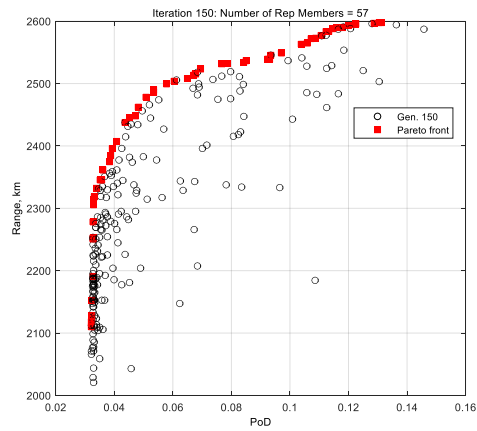
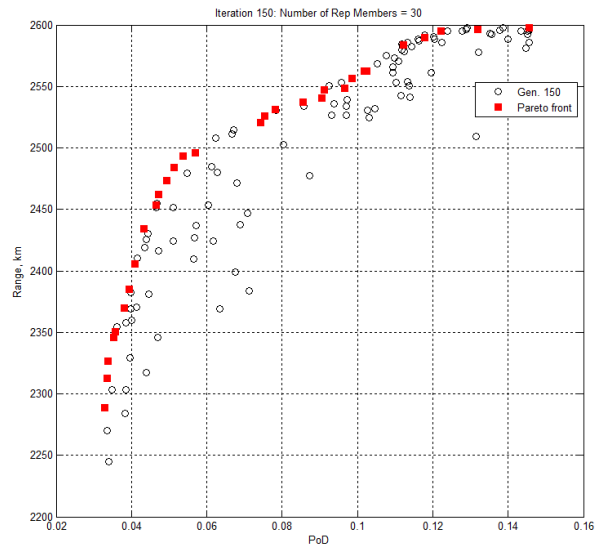


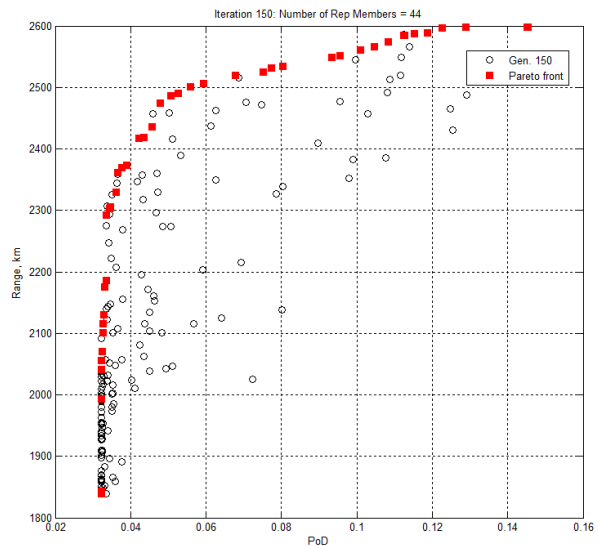
Figure 3.2 Trials for maximum number of iteration. a) Iteration: 60, b) Iteration: 80, c) Iteration: 100, d) Iteration: 120, e) Iteration: 150

The effect of population size to Pareto front results is also examined. The examination was carried out for 100, 150 and 200 number of members when maximum iteration and repository size set fixed respectively as 150 and %30 of population size. As seen in Figure 3.3, for low population size that includes 100 members, Pareto front results are not enough to cover real Pareto front. The more increase in the population size, the more the resolution of Pareto results increase. However, to prevent the increase of computational time, 200 number of members are enough to reach a good Pareto front.

a)



b)



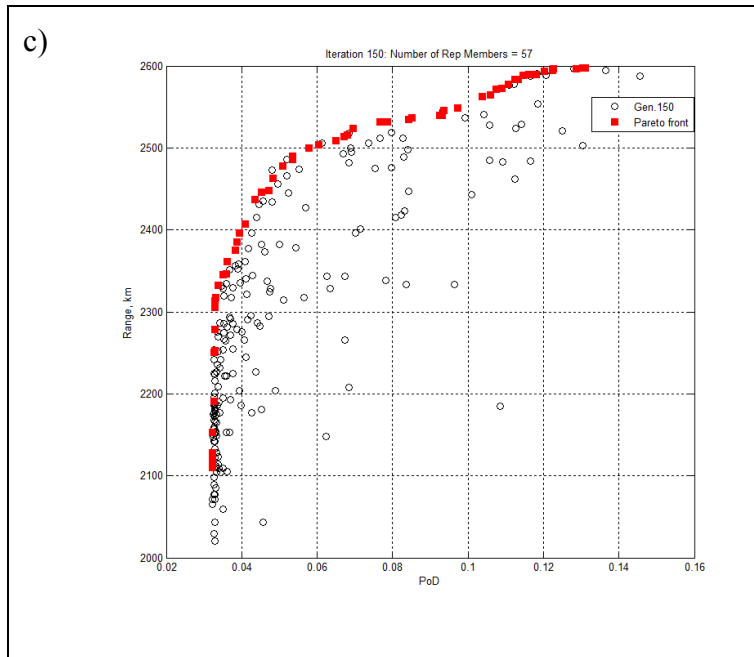


Figure 3.3 Trials for population size. a) Population size: 100 individuals, b) Population size: 150 individuals, c) Population size: 200 individuals

The effects of optimization parameters to Pareto front were evaluated. As a result of this, the population size of the swarm is defined as 200 individuals. The maximum number of iteration (or generation) is chosen as 120. The repository size set to 80 individuals.

### 3.2 Discussions

The optimization framework was run with defined parameters. The Pareto front solutions can be seen Figure 3.4. Here, results of multi-objective multidisciplinary design problem will be evaluated.

The change of the geometry planform from minimum Possibility of Detection (PoD) to maximum Range can be shown in Table 3.2. There are 80 members defined as Pareto front solutions. “Rep\_1” represent the repository member, which has minimum PoD value, and range increases from “Rep\_1” to “Rep\_80” as the PoD increases. In Figure 3.5, the change of geometry variables are also illustrated in order

to bring out which variables are more effective at trade-off between minimum PoD and maximum range. When the behavior of the change of geometry planform over Pareto is considered, it is seen that geometry planform decreases its total span and sweep angle values and increases root chord length ( $c_1$ ) to minimize PoD value. To maximize range, geometry planform goes to high sweep angles and increasing span. When sweep angle of geometry increases, lift-to-drag ratio increases. The one reason of this situation can be explained that the effect of tip vortices on body of geometry decrease when sweep angle increases. The main reason, here, is that with increasing sweep angle, compressibility effects decrease in transonic speeds [35]. This means that significant drop in drag is occurred with increasing sweep angle.

When we consider the behavior of Pareto front curve, PoD values of repository members don't change much between PoD = 0.032 and PoD 0.05 while range increases dramatically. After this point, Pareto front curve acts in an opposite trend. Therefore, a point around Range equals or greater than 2500 km can be chosen as design point. For example, "Rep\_50" is considered as design points and its detailed specification is given in Table 3.3. RCS signature of "Rep\_50" is also illustrated in Figure 3.7.

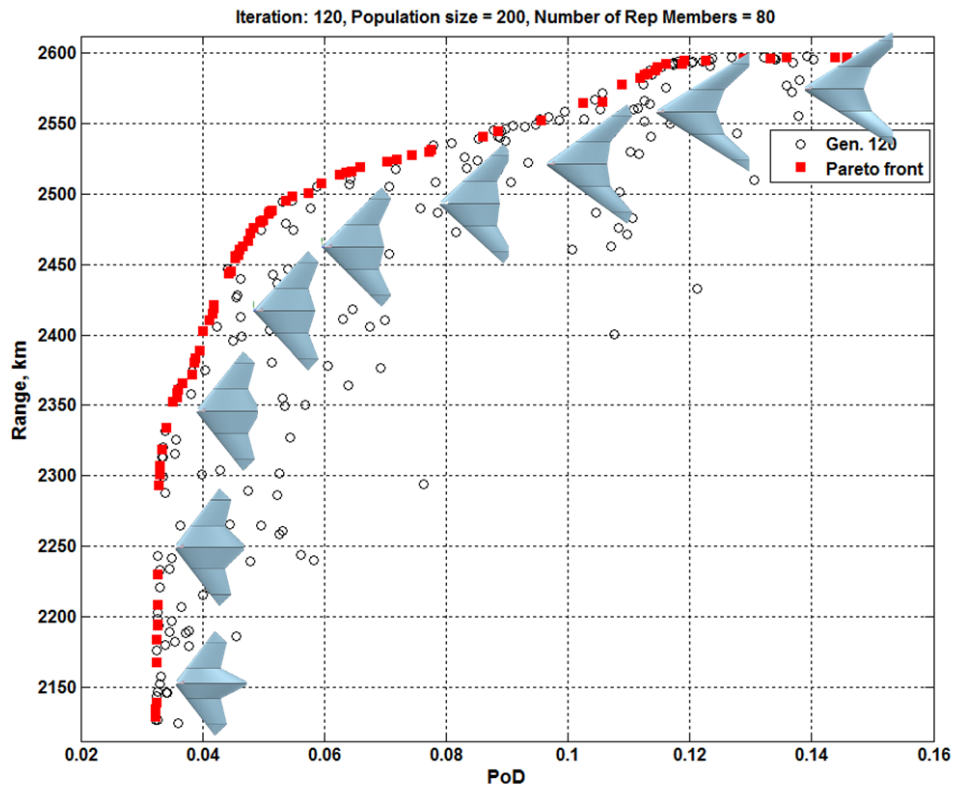


Figure 3.4 Pareto front solutions for optimization framework

Table 3.2 Change of geometry planform from min. PoD to max. Range

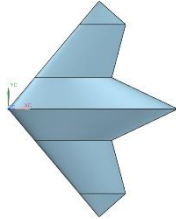
<p>Rep_1</p> <p>PoD= 0,0322</p> <p>Range=2129 km</p>	
--	--

Table 3.2 Change of geometry planform from min. PoD to max. Range (cont'd)

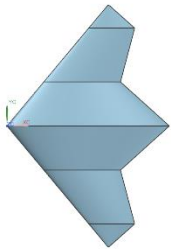
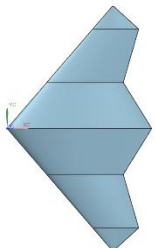
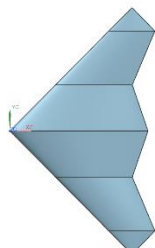
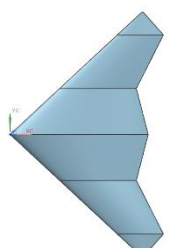
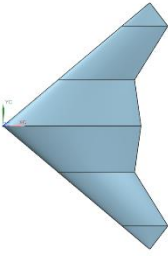
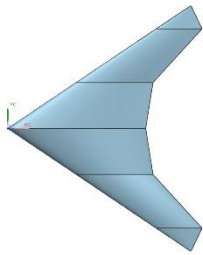
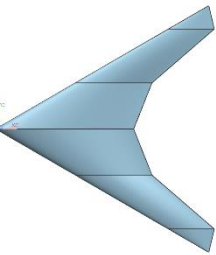
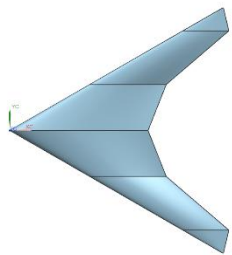
<p>Rep_10 PoD= 0,0329 Range=2293 km</p>	
<p>Rep_20 PoD= 0,0367 Range=2365 km</p>	
<p>Rep_30 PoD= 0,0443 Range=2443 km</p>	
<p>Rep_40 PoD= 0,0484 Range=2475 km</p>	

Table 3.2 Change of geometry planform from min. PoD to max. Range (cont'd)

<p>Rep_50 PoD= 0,0594 Range=2507 km</p>	
<p>Rep_60 PoD= 0,0860 Range=2540 km</p>	
<p>Rep_70 PoD= 0,1145 Range=2590 km</p>	
<p>Rep_80 PoD= 0,1456 Range=2597 km</p>	

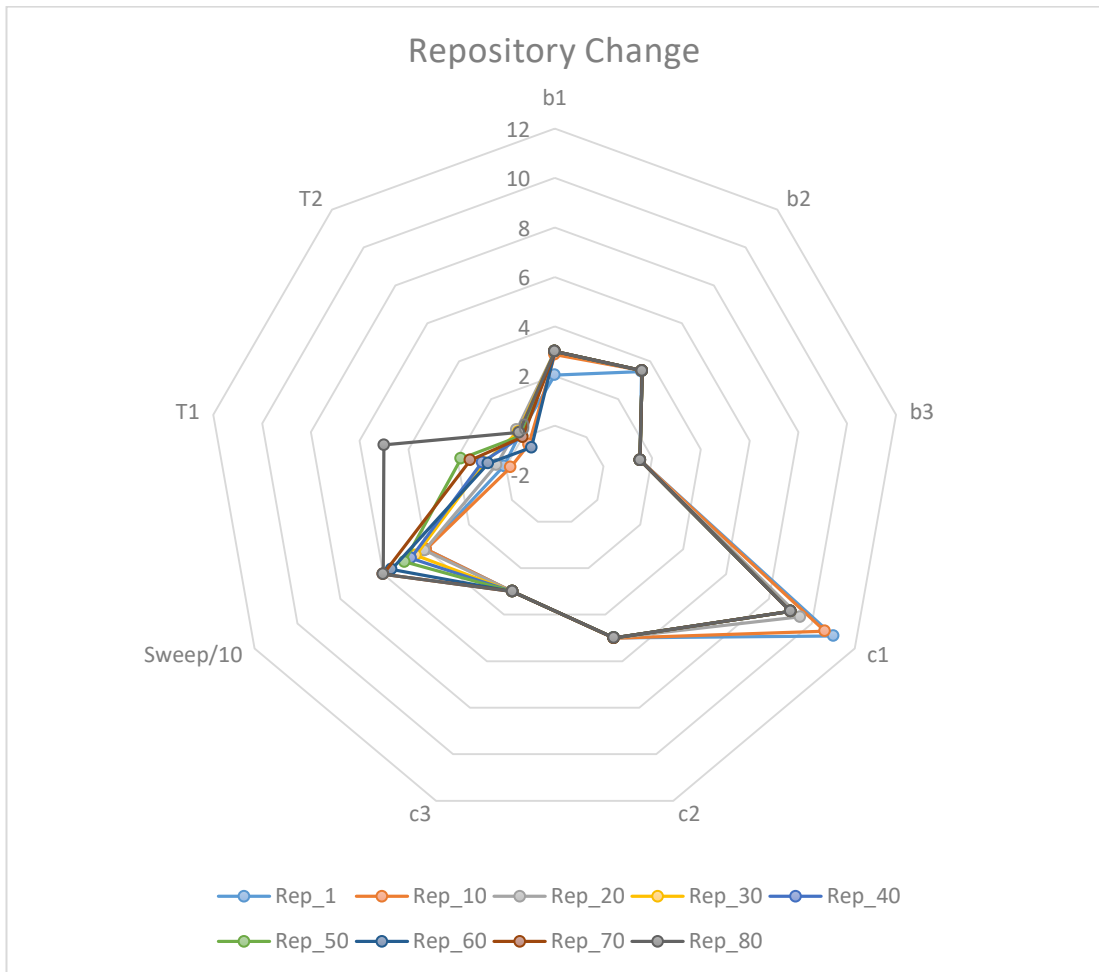


Figure 3.5 Change of geometry variables from min. PoD (Rep\_1) to max. Range (Rep\_80)

Table 3.3 Specifications of design point “Rep\_50” geometry

Geometry Spec.		Aircraft Mass Spec.		Aerodynamic Spec.	
Span Length (B1)	3,0	Total Mass, kg	10672	Sref, m <sup>2</sup>	74,46
Span Length (B2)	3,5	Empty Mass, kg	5471	MAC, m	5,71
Span Length (B3)	1,5	Structure Mass, kg	2321	Bref, m	15,99
Chord Length (C1)	9,0	System Mass, kg	1281	Lift-to-Drag ratio	19,90
Chord Length (C2)	5,0	Payload Mass, kg	2000	<b>Engine Spec.</b>	
Chord Length (C3)	3,0	Engine Mass, kg	898	SFC, 1/hr	0,78
Leading Edge Sweep ( $\Lambda$ )	50,0	Fuel Mass, kg	3202	MaxThrustReq, kg	3842
Twist Angle ( $\Theta_2$ )	1,8				
Twist Angle ( $\Theta_3$ )	0,1				

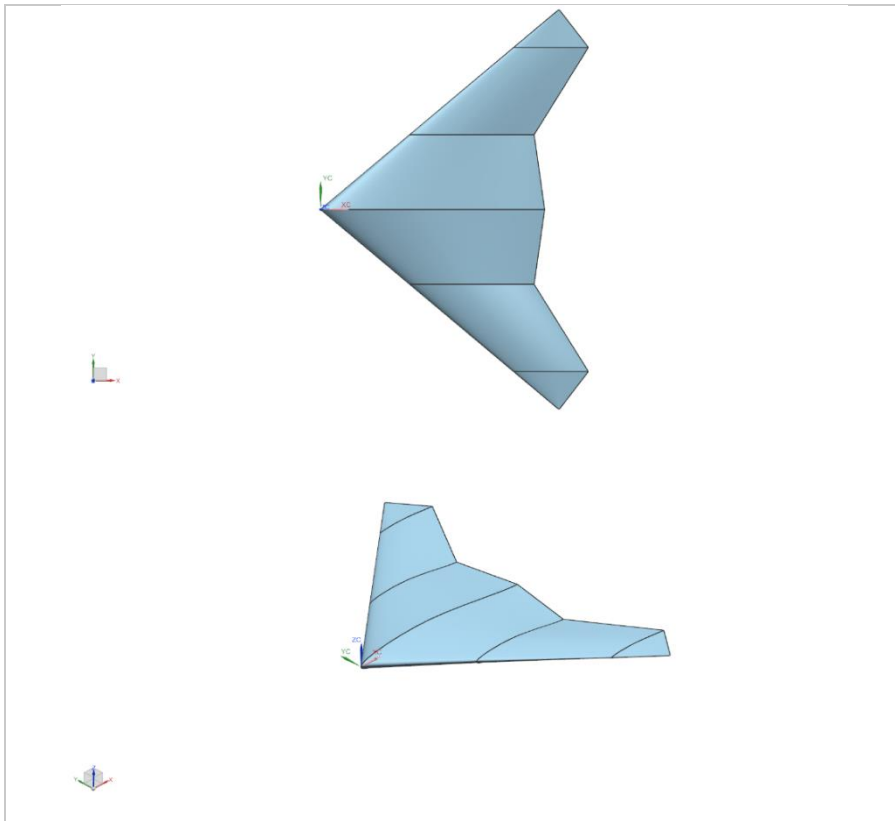


Figure 3.6 3D view of “Rep\_50” geometry

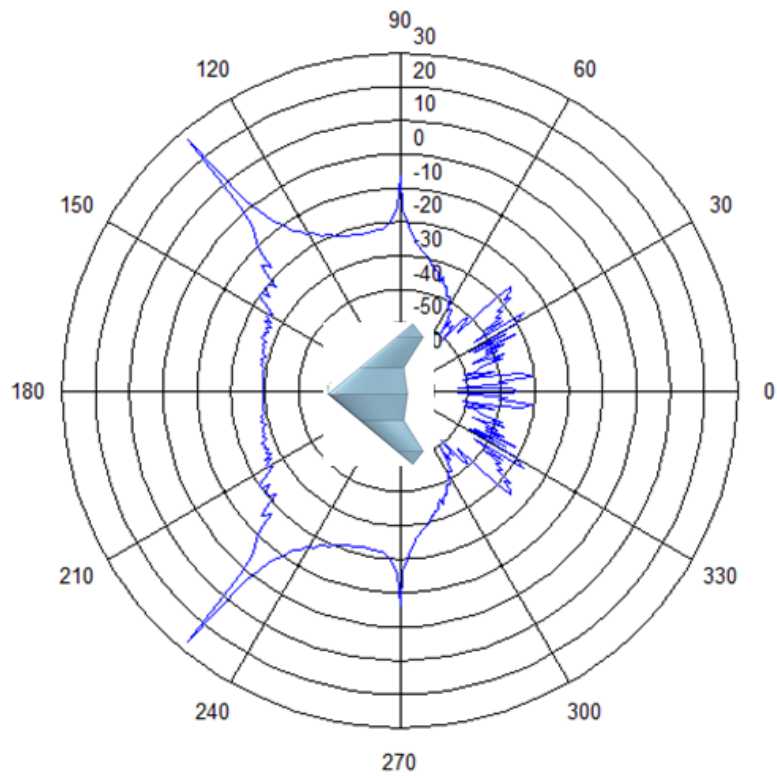


Figure 3.7 RCS signature of Rep\_50 in dBm



## CHAPTER 4

### CONCLUSIONS AND FUTURE WORK

#### 4.1 Conclusions

In this thesis, multi-disciplinary design optimization framework was developed to manage the conceptual design process of Unmanned Combat Aerial Vehicle (UCAV). This framework consists of modules for generating 3D geometry, analysis of aerodynamics and RCS signature, weight estimation, performance calculation and optimization.

The chosen geometry was parameterized to define the design variables of optimization problem. The SACCON 1303 shape given in Ref [6] was considered as a baseline planform in this study. Analysis of aerodynamics, weight estimation and radar cross section (RCS) signature were employed in the framework. Aerodynamic analysis was performed using SU2 Euler solver. Flight conditions for aerodynamic analysis were defined that aircraft flies with Mach 0.8 velocity and at 11 km altitude. Moreover, to shorten computational effort, a meta-model for aerodynamic results is formed by performing multivariate adaptive regression splines (MARS) approximation. Weight estimation was employed using empirical and statistical equations. RCS signature was calculated using POFACETS which is an implementation of the physical optics approximation. The RCS signature calculation was monostatically executed in xy plane of aircraft body frame. Also, meta-model of RCS results was generated to decrease the computational time. Maximum cruise range and minimum RCS signature were employed as objective functions. Multi-objective particle swarm optimization (MOPSO) was performed to generate Pareto-optimal solutions.

The population size of the swarm was defined as 200 individuals. The maximum number of iteration (or generation) was chosen as 120. The repository size

set to 80 individuals. The optimization framework was run with these parameters. The Pareto front solutions show that geometry planform decreases its total span and sweep angle values and increases root chord length ( $c_1$ ) to minimize PoD value. Also, planform goes to high sweep angles and increasing span to maximize cruise range with increasing lift-to-drag ratio. This can be explained with that the effect of tip vortex on body of geometry decreases when sweep angle increases. Moreover, increasing sweep angle decrease compressibility effects in transonic speeds. Therefore, drag to lift ratio increases for same lift. Although the Pareto members with highly swept wings have greater lift-to-drag ratio, these geometries will suffer from longitudinal stability because of high pitching moment. Also, structural constraints and requirements are not included in the design framework. When the Pareto optimal geometries are considered according to structural point of view, it can be said that the region near the minimum RCS and maximum Range in Pareto front curve might not be feasible solution.

As a represent of the study, 50<sup>th</sup> member of repository were depicted with detailed specifications in Figure 3.7 and Figure 3.8. The planform shape is similar to competitor UCAVs like Neuron and Taranis.

In conclusion, the multi-disciplinary design optimization framework consisted of submodules was developed to find to optimal design points for the UCAV. The low fidelity tools and methods were used to estimate aerodynamics, RCS signature and maximum total weight in this framework. The meta-modeling technique was utilized to reduce computational cost of expensive simulation. Multi-objective optimization was employed to understand the trade-off between multiple requirements. As a result of this study, automated process was generated to manage the conceptual design process.

## 4.2 Future Work

This study is the demonstration of how MDO framework can improve aircraft conceptual design. The widest possible design space can be explored with MDO framework. MDO techniques truly can improve the weight and cost of an aircraft design concept in the conceptual design phase.

It is easy to increase the capability and fidelity of the framework with the addition of new modules to the framework or replacement of modules with others. Therefore, in the future, more disciplines like structural analysis, flight mission analysis, weight-balance and flight stability can be added to the framework. For example, structural layout of the UCAV geometry can be defined basically using automated 3D CAD (Computer Aided Design) tool by number and position of spars and ribs within structural analysis module. Moreover, interior volume calculation and weight estimation for the required fuel and structural weight estimation can be done more easily and accurately with these capabilities. Instead of fixed fuel weight fraction, detailed mission simulation could be integrated into the framework and the required fuel weight estimation can be done more accurately.

The fidelity level of current modules like aerodynamics, RCS and weight estimation can be increased by replacing them with new methods. For example, instead of using the Euler solver, the RANS solver can be adopted to the meta-modeling process.

Different objective functions or performance parameters can be considered with different constraints in the future. Different optimization methods can be used to find the optimal solutions. For example, both the gradient-based and the gradient-free optimization methods can be employed to the framework and the performance of these methods can be compared. As a conclusion, the limits are endless.



## REFERENCES

- [1] Me. Joe Coppin, “Aerodynamics, Stability and Shape Optimisation of Unmanned Combat Air Vehicles,” no. September, p. 172, 2014.
- [2] “Taranis-490x326.jpg (490×326).” [Online]. Available: <https://www.defensetech.org/wp-content/uploads/2014/07/Taranis-490x326.jpg>. [Accessed: 10-Dec-2017].
- [3] “8-2015-4\_neuron\_stealth\_test\_flights\_.jpg (2500×1674).” [Online]. Available: [https://www.ainonline.com/sites/default/files/uploads/2015/08/8-2015-4\\_neuron\\_stealth\\_test\\_flights\\_.jpg](https://www.ainonline.com/sites/default/files/uploads/2015/08/8-2015-4_neuron_stealth_test_flights_.jpg). [Accessed: 10-Dec-2017].
- [4] “the-x-47b-drone-plane-can-carry-4500-pounds-of-weapons-and-operate-all-on-its-own.jpg (940×705).” [Online]. Available: <http://static5.businessinsider.com/image/4f217edaeab8ea110d00000b/the-x-47b-drone-plane-can-carry-4500-pounds-of-weapons-and-operate-all-on-its-own.jpg>. [Accessed: 10-Dec-2017].
- [5] “00003837\_medium.jpeg (639×431).” [Online]. Available: [http://pix.avaxnews.com/avaxnews/37/38/00003837\\_medium.jpeg](http://pix.avaxnews.com/avaxnews/37/38/00003837_medium.jpeg). [Accessed: 10-Dec-2017].
- [6] C. M. Liersch, K. C. Huber, A. Schütte, M. Rein, and T. Löser, “Multidisciplinary Design and Aerodynamic Assessment of an Agile and Highly Swept Aircraft Configuration,” *CEAS Aeronaut. J.*, vol. 7, no. 4, pp. 677–694, 2016.
- [7] R. M. Cummings and A. Schutte, “An Integrated Computational/Experimental Approach to UCAV Stability & Control Estimation: Overview of NATO RTO AVT-161,” *AIAA Appl. Aerodyn. Conf.*, no. July, pp. 1–23, 2010.
- [8] S. J. Woolvin *et al.*, “UCAV Configuration & Performance Trade-Offs,” *Technology*, no. January, pp. 1–14, 2006.
- [9] H. Tianyuan and Y. Xiongqing, “Aerodynamic/Stealthy/Structural Multidisciplinary Design Optimization of Unmanned Combat Air Vehicle,” *Chinese J. Aeronaut.*, vol. 22, no. 4, pp. 380–386, 2009.

- [10] A. Sathe and R. S. Pant, "Conceptual Design Studies of an Unmanned Combat Aerial Vehicle, AIAA 2010-9306," *10th AIAA Aviat. Technol. Integr. Oper. Conf. Fort Worth, Texas 13-15 Sept.*, no. September, pp. 1–10, 2010.
- [11] N. Nguyen, S. Choi, W. Kim, K. Jeon, J. Lee, and Y. Byun, "Multidisciplinary Unmanned Combat Air Vehicle-UCAV Design Optimization Using Variable Complexity Modeling," *9th AIAA Aviat. Technol. Integr. Oper. Conf.*, no. September, pp. 1–14, 2009.
- [12] R. Vos and J. Van Dommelen, "A Conceptual Design and Optimization Method for Blended-Wing-Body Aircraft," *53rd AIAA/ASME/ASCE/AHS/ASC Struct. Struct. Dyn. Mater. Conf.*, no. April, pp. 1–14, 2012.
- [13] D. P. Raymer, "Enhancing Aircraft Conceptual Design Using Multidisciplinary Optimization," 2002.
- [14] A. Papageorgiou, "Development of a Multidisciplinary Design Optimization Framework applied on UAV Design."
- [15] C. Optimization, K. Amadori, C. Jouannet, and P. Krus, "Use of Panel Code Modeling in a Framework for Aircraft Concept Optimization," *11th AIAA/ISSMO Multidiscip. Anal. Optim. Conf.*, no. September, pp. 1–13, 2006.
- [16] O. Gur, W. H. Mason, and J. A. Schetz, "Full-Configuration Drag Estimation," *J. Aircr.*, vol. 47, no. 4, pp. 1356–1367, 2010.
- [17] E. Garrido, "Graphical user interface for a physical optics radar cross section prediction code," Naval Postgraduate School, 2000.
- [18] F. Chatzigeorgiadis, "Development of Code For a Physical Optics Radar Cross Section Prediction and Analysis Application," Naval Postgraduate School, 2004.
- [19] J. D. Anderson, "Aircraft Performance and Design," *Encyclopedia of Physical Science and Technology (Third Edition)*. pp. 365–397, 2003.
- [20] C. A. Coello Coello and M. S. Lechuga, "MOPSO: A proposal for multiple objective particle swarm optimization," *Proc. 2002 Congr. Evol. Comput. CEC 2002*, vol. 2, pp. 1051–1056, 2002.
- [21] T. Melin, "A vortex lattice MATLAB implementation for linear aerodynamic

- wing applications,” 2000.
- [22] D. Lynch, *Introduction to RF Stealth*. 2003.
- [23] B. Persson, *Assessment of Aircraft Radar Cross-Section for Detection Analysis*. 2016.
- [24] W. L. Stutzman and G. A. T. Thiele, *Antenna Theory Analysis and Design Third Edition*, no. 3. 2005.
- [25] R. Shevell, *Fundamentals of Flight*, no. May. 1998.
- [26] D. Howe, *Aircraft conceptual design synthesis*. 2000.
- [27] A. S. Walker, “Development of a Conceptual Flight Vehicle Design,” no. May, 2014.
- [28] K. E. Parsopoulos and M. N. Vrahatis, “Multi-Objective Particles Swarm Optimization Approaches,” *Multi-Objective Optim. Comput. Intell.*, pp. 20–42.
- [29] C. a. C. Coello, D. a. Van Veldhuizen, and G. B. Lamont, *Evolutionary Algorithms for Solving Multi-Objective Problems (Genetic and Evolutionary Computation)*. 2002.
- [30] D. Kunkle, “A summary and comparison of MOEA algorithms,” *Northeast Univ. Boston, Massachusetts*, vol. 2, no. 2003, pp. 1–19, 2005.
- [31] M. Köppen, R. Verschae, K. Yoshida, and M. Tsuru, “Comparison of evolutionary multi-objective optimization algorithms for the utilization of fairness in network control,” *Conf. Proc. - IEEE Int. Conf. Syst. Man Cybern.*, pp. 2647–2655, 2010.
- [32] “Fugle\_ørnsø\_073.jpg (2048×1536).” [Online]. Available: [https://upload.wikimedia.org/wikipedia/commons/d/d6/Fugle%2C\\_ørnsø\\_073.jpg](https://upload.wikimedia.org/wikipedia/commons/d/d6/Fugle%2C_ørnsø_073.jpg). [Accessed: 10-Dec-2017].
- [33] D. W. Corne, J. D. Knowles, and M. J. Oates, “The Pareto Envelope-based Selection algorithm for Multiobjective Optimization,” vol. XXXIII, no. 2, pp. 81–87, 2012.
- [34] J. Durillo and J. García-Nieto, “Multi-objective particle swarm optimizers: An experimental comparison,” *5th Int. Conf. EMO 2009*, pp. 495–509, 2009.

- [35] R. Vos and S. Farokhi, *Introduction to Transonic Aerodynamics*, vol. 110. 2015.
- [36] T. W. Simpson, J. D. Peplinski, P. N. Koch, and J. K. Allen, “On the use of statistics in design and the implications for deterministic computer experiments,” *Proc. DETC’97 1997 ASME Des. Eng. Tech. Conf.*, no. February, pp. 1–14, 1997.
- [37] R. Jin, W. Chen, and T. W. Simpson, “Comparative studies of metamodelling techniques under multiple modelling criteria,” *Struct. Multidiscip. Optim.*, vol. 23, no. 1, pp. 1–13, 2001.
- [38] M. Statistics, “Multivariate Adaptive Regression Splines Author ( s ): Jerome H . Friedman Source : The Annals of Statistics , Vol . 19 , No . 1 ( Mar . , 1991 ), pp . 1-67 Published by : Institute of Mathematical Statistics Stable URL : <http://www.jstor.org/stable/224183>,” vol. 19, no. 1, pp. 1–67, 2017.
- [39] A. I. J. Forrester, A. Sóbester, and A. J. Keane, *Engineering Design via Surrogate Models*. 2008.
- [40] M. D. Morris and T. J. Mitchell, “Exploratory designs for computational experiments,” *J. Stat. Plan. Inference*, vol. 43, no. 3, pp. 381–402, 1995.

## APPENDIX A

### META-MODELLING TECHNIQUE

Meta-modeling is preferable strategy to utilize approximation models for complex and high fidelity simulations. Meta-modeling techniques have been used for design optimization in many areas from aerospace applications to mechanical applications [36]. There are a variety of meta-modeling methods; response surface methodology, artificial neural network, kriging methods, radial basis function and multivariate adaptive regression splines. In study of Simpson, et al, comparison of four meta-modeling techniques, which are polynomial regression, kriging, multivariate adaptive regression splines and radial basis functions, are evaluated with accuracy and robustness, efficiency, transparency and simplicity. MARS is performed as the best for the most difficult problems, i.e., large-scale and high-order nonlinear problems when accuracy and robustness are both considered [37]. Therefore, MARS is chosen as the meta-modeling technique to be used in Aerodynamics and RCS modules.

In Multivariate Adaptive Regression Splines (MARS), a set of basis functions is adaptively selected for approximating the response function through a forward/backward iterative approach [38].

Equation of MARS can be expressed as:

$$\hat{y} = \sum_{m=1}^M \alpha_m \beta_m(x) \quad (\text{A.1})$$

where  $\alpha_m$  is the coefficient of the expansion, and  $\beta_m$  is the basis function.  $\beta_m$  can be represented as:

$$\beta_m(x) = \prod_{k=1}^{K_m} [s_{k,m}(x_{v(k,m)} - t_{k,m})]_+^q \quad (\text{A.2})$$

Where  $K_m$  is the number of factors in the  $m$ -th basis function,  $s_{k,m} = \pm 1$ ,  $x_{v(k,m)}$  is the  $v$ -th variable,  $1 \leq v(k,m) \leq n$ , and  $t_{k,m}$  is a knot location on each of the corresponding variables. The subscript ‘+’ means the function is a truncated power function.

$$[s_{k,m}(x_{v(k,m)} - t_{k,m})]_+^q = \begin{cases} [s_{k,m}(x_{v(k,m)} - t_{k,m})]^q & ; s_{k,m}(x_{v(k,m)} - t_{k,m}) < 0 \\ 0 & ; otherwise \end{cases} \quad (\text{A.3})$$

MARS model building procedure is can be summarize as below:

<b>MARS model building procedure</b>
<ol style="list-style-type: none"> <li>1. Gather data - x input variables with y observations</li> <li>2. Calculate set of candidate functions by generating reflected pairs of basis functions with knots set at observed values.</li> <li>3. Specify constraints - the number of terms in the model and maximum allowable degree of interaction.</li> <li>4. Do forward pass - Try out new function products and see which product decreases training error.</li> <li>5. Do backward pass - Fix overfit.</li> <li>6. Do generalized cross validation to estimate the optimal number of terms in the model.</li> </ol>

Sampling plan must be considered to create meta-model more precisely and more efficiently. In this study, Optimized Latin Hypercubes method is used as sampling strategy.

In Latin Hypercubes methods, design space is splitting into equal sized hypercubes (bins) and placing points in the hypercubes, making sure that from each occupied bin we could exit the design space along any direction parallel with any of the axes without encountering any other occupied bins [39]. Example for three dimensional Latin hypercube sampling plan is shown in Figure A.1.

In Optimized Latin Hypercubes, “space-fillingnes” metric is optimized to distribute sample points uniformly in design space. This metric, introduced by Morris and Mitchell, is used as a measure to evaluate the uniformity of sampling plan. Morris and Mitchell define a scalar-valued criterion function as [40]:

$$\Phi_q(X) = \left( \sum_{j=1}^m J_j d_j^{-q} \right)^{1/q} \quad (0.4)$$

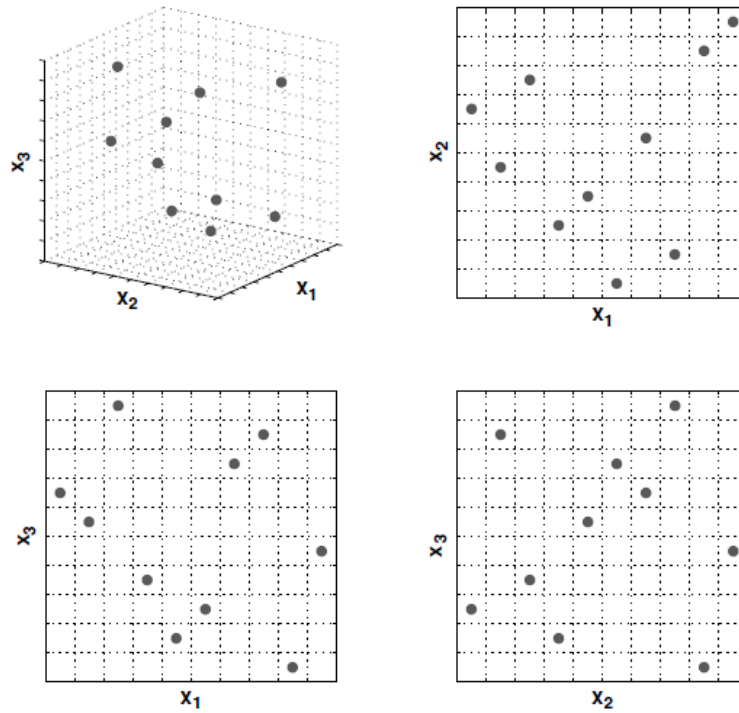


Figure A.1 Three-variable, ten-point Latin hypercube sampling plan shown in three dimensions (top left), along with its two-dimensional projections [39].

Where,  $d_j$  list of the unique values of distances between all possible pairs of points in a sampling plan  $X$  and  $J_j$  is the number of pairs of points in  $X$  separated by the distance  $d_j$ . The space-filling properties of sampling plan ( $X$ ) will be better, when the value of  $\Phi_q$  is smaller. In optimization process, the evolutionary operation is

used and best of the optima found for the various  $q$ 's is selected. Therefore, the design of experiment is generated for given design space.

In here, meta-modelling technique, MARS, and sampling plan method used in this study was explained with general details. For more information about meta-modelling and sampling plan, Ref. [36]–[39] can be examined.

In order to measure the error between real model and the metamodel, Root Mean Square Error (RMSE) method is used. The formula to calculate RMSE can be seen in below. In order to evaluate the accuracy of the metamodel with RMSE parameters, RMSE also has to be normalized with dividing by the mean value of real models values. For Normalized RMSE less than %10, meta-model can be acceptable as a good model and for Normalized RMSE less than %2, meta-model yield a very good model [39].

$$RMSE = \sqrt{\frac{\sum_{i=1}^n (X_{real_i} - X_{metamodel_i})^2}{n}} \quad (A.5)$$

$$NRMSE = \frac{RMSE}{\overline{X_{real}}} \quad (A.6)$$

## APPENDIX B

### VALIDATION OF MOPSO ALGORITHM FOR MULTIDISCIPLINARY OPTIMIZATION PROBLEM

To validate that the MOPSO method is good enough to find true Pareto front results, some test function was run with the MOPSO method. Here, MOP2 and ZDT1 functions given in the Ref [29] were used as the test functions. The test functions can be found in the Table B.1. The results of these runs and true Pareto-optimal front presented in Ref [29] are compared in Figure B.1. As can be seen in the Figure B.1, Pareto front results of MOPSO and true Pareto front are similar for both ZDT1 and MOP2 test functions.

Table B.1 Formulations of ZDT1 and MOP2 test functions

ZDT1 Test Function	$f_1(x) = x_1$ $f_2(x, g) = g(x) \cdot (1 - \sqrt{f_1/g(x)})$ $g(x) = 1 + \frac{9}{n-1} \cdot \sum_{i=2}^n x_i$ <p><i>Minimize:</i> <math>F(x) = (f_1, f_2)</math>            where <math>n = 30</math> and <math>x_i \in [0,1]</math></p>
MOP2 Test Function	$f_1(x) = 1 - \exp\left(-\sum_{i=1}^n \left(x_i - \frac{1}{\sqrt{n}}\right)^2\right)$ $f_2(x) = 1 - \exp\left(-\sum_{i=1}^n \left(x_i - \frac{1}{\sqrt{n}}\right)^2\right)$ <p><i>Minimize:</i> <math>F(x) = (f_1, f_2)</math>            where <math>n = 3</math> and <math>x_i \in [-4,4]</math></p>

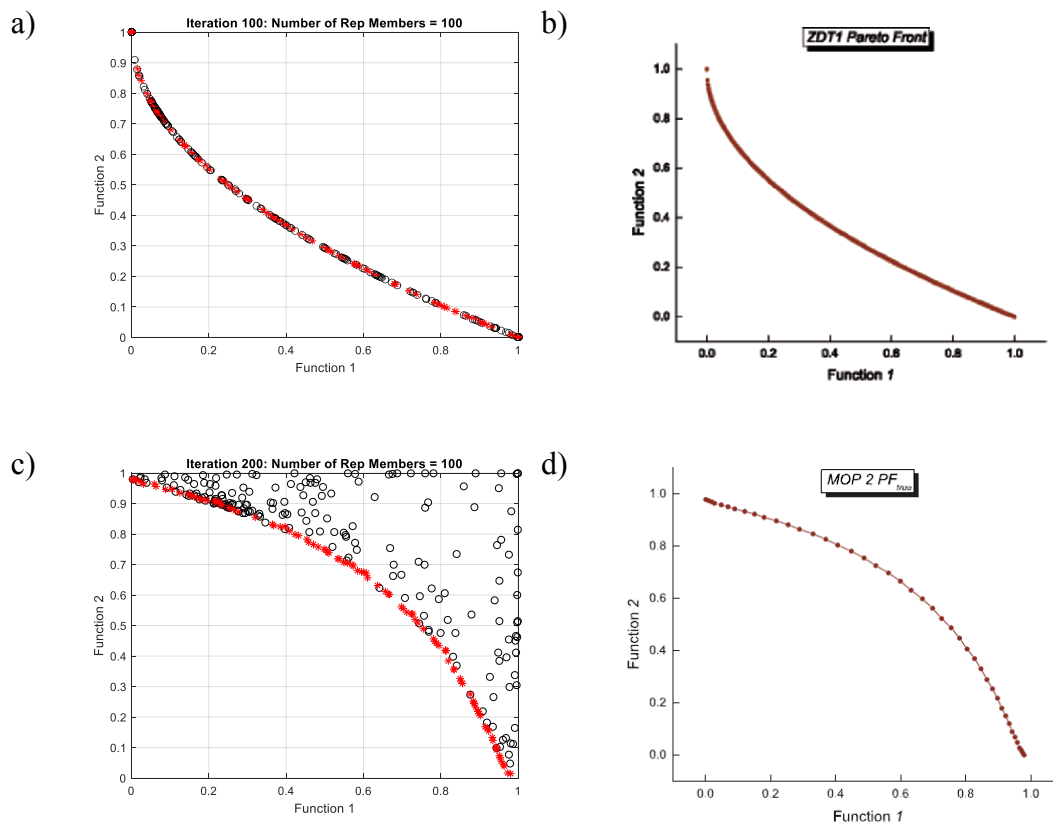


Figure B.1 Validation of MOPSO algorithm. a) MOPSO results for ZDT1 test function, b) true Pareto front for ZDT1 test function [29], c) MOPSO results for MOP2 test function, d) true Pareto front for MOP2 test function [29]